

https://dspace.org/

Electrical conduction in carbon-ion implanted diamond and other materials at low temperatures.

Tshepe, Tshakane Frans

1992
https://hdl.handle.net/10539/26299

Downloaded from a DSpace repository. https://dspace.org/

ELECTRICAL CONDUCTION IN CARBON-ION IMPLANTED DIAMOND AND OTHER MATERIALS AT LOW TEMPERATURES

Tshakane Frans Tshepe

A research report submitted to the Faculty of Science, University of the Witwatersrand, Johannesburg, in partial fulfilment of the requirements for the degree of Master of Science

Johannesburg

December 1992

ABSTRACT

The role of intersite electron correlation effects and the possible occurrence of the metal-insulator transition in carbon-ion implanted type IIa diamond samples have been studied at very low temperatures, using four- and two-point probe contact electrical conductivity measuring techniques. The measurements were extended to ruthenium oxide thin films in the presence and absence of a constant magnetic field of $\mathbf{B} = 4.0$ T down to 100 mK, using a ^{3}He-^{4}He dilution refrigerator. The effect of the Coulomb gap in the variable range hopping regime has been well studied by other workers. The results tend to follow the Efros-Shklovskii behaviour with a trend towards the Mott $T^{-1/4}$ law for diamond samples far removed from the metal insulator transition, on the insulating side at low temperatures.

DECLARATION

I declare that this research report is my own, unaided work. It is being submitted for the degree of Master of Science to the University of the Witwatersrand, Johannesburg. It has not been submitted before for any degree or examination in any university.

Signed : _____
(Tshakane Frans Tshepe)

23th day of December 1992

In Memory of my Mother

Nkgathi Justina Tshepe

1935-1973

ACKNOWLEDGEMENTS

I am deeply indebted to my supervisor Prof M.J.R. Hoch for giving me the opportunity and freedom to learn and grow under his guidance. He has made me see through the dark glasses of my limitations, by building self-confidence and self-reliance in me.

I wish to express my sincere gratitude to Prof D.S. McLachlan, and Dr J.F. Prins for devoting their most valuable time in making this project a success. Many thanks are due also to my colleagues, Mr Ncholu Manyala and Mr Ike Sikakana, for discussions of part of the research report.

The university senior bursary and Daad Funding schemes are thanked for their generous financial support.

CONTENTS

List of Figures ix

List of Tables x

Chapter 1. General Introduction 1

1.1 Introduction 1

1.2 Conduction in Diamond 2

1.3 A report on Ruthenium Oxide Thin Films 3

1.4 The Scope of the Research Report 5

1.5 Outline of the Research Report 6

Chapter 2. Theory of Hopping Conduction in Heavily Doped Semiconductors at Low Temperatures 7

2.1 Introduction 7

2.2 Anderson Localization 8

2.3 Mott and Efros-Shklovskii Conduction Theory 12

2.4 Coulomb Gap 14

2.5 Demonstration of the Coulomb Gap 14

2.6 Effect of the Coulomb Gap 17

Chapter 3. Experimental Details 18

3.1 General Considerations 18

3.2 Lattice disorder 18
3.3 Range Distribution of the Implanted Atoms 19
3.4 Lattice Location and Electrical Properties 21
3.5 Ion Implantation in Diamond Samples 21
3.6 Sample Preparation 22
3.7 Sample Cleaning 24
3.8 Sample Mounting 24
3.9 Electrical Contacts 25
3.10 Measuring Procedure 27
3.11 Fitting Procedure to Experimental Data 30

Chapter 4. Experimental Results 34

4.1 Diamond Results 34
4.2 Results of Two-point Probe Contacts 37
4.3 Results of RuO_2 Thin Films 41

Chapter 5. Discussion of the Results 44

5.1 Introduction 44
5.2. Sample Discussion 44
5.2.1 *Sample 3 (Weak Hopper* - 5.85×10^{15} cm^{-2}) 44
5.2.2 *Sample 2 (Mild Hopper* - 5.70×10^{15} cm^{-2}) 46
5.2.3 *Sample 1 (Strong Hopper* - 5.65×10^{15} cm^{-2}) 46
5.3 Hopping Conduction in Doped Semiconductors 47
5.4 Excitation in the Coulomb Gap 48
5.5 Discussion of Two-point Probe Contact Measurements 50
5.6 Discussion of RuO_2 Results 51

Chapter 6. Summary and Conclusion 52

6.1 Type IIa Diamond Results 52

6.2 RuO_2 Thin film Results 53

References 54

Appendix 59

LIST OF FIGURES

Figure 1.1 Plot of $\rho(\Omega\ \text{cm})$ against $T^{-1/4}$ for carbon-ion implanted type IIa diamond from 330 K to 20 K 4

Figure 2.1 Crystalline and random potentials with corresponding density of states. The wavefunction ψ of an electron in a weakly localized state 10

Figure 2.2 Density of states in an Anderson band with two mobility edges E_c and $E_{c'}$. The shaded states are localized. 11

Figure 2.3 Depiction of the effect of the shape of the density of states 16

Figure 3.1 Diamond type structure showing (a) $< 100 >$ axial orientation and (b) 'random' direction at $10°$ from $< 110 >$ 20

Figure 3.2 Sample holder used to mount diamond samples 26

Figure 3.3 Dip stick used to mount samples into a liquid ^{4}He dewar 28

Figure 3.4 Schematic view of copper contacts on a diamond sample 29

Figure 3.5 (a) Plot of $\ln W$ vs $\ln \overline{T}$ for a mild hopper
(b) Plot of $\frac{\partial \ln g}{\partial \ln T}$ vs $\ln g$ for a mild hopper 32

Figure 4.1 Plot of log (Res) vs Implantation dose for diamond samples at different temperatures 35

Figure 4.2 Plot of log (Res (Ω)) vs T (K) for diamond samples 36

Figure 4.3 Plot of log (Res (Ω)) vs T^{-n} (K^{-n}) for a weak hopper 38

Figure 4.4 Plot of log (Res (Ω)) vs T^{-n} (K^{-n}) for a mild hopper 39

Figure 4.5 Plot of log (Res (Ω)) vs T^{-n} (K^{-n}) for a strong hopper 40

Figure 4.6 Plot of log (Res (Ω)) vs T^{-n} (K^{-n}) 42

Figure 4.7 Plot of log (Res (Ω)) vs T^{-n} (K^{-n}) for 1 KΩ ruthenium oxide thin films 43

LIST OF TABLES

Table 3.1 Energies at which carbon ions were accelerated into diamond at nitrogen temperatures. These values were determined from TRIM 89 23

Table 5.1 Estimated optimum hop distances for mild and strong hoppers at different temperatures 49

Table 5.2 Results of mild and strong hoppers that characterize the low temperature conductivity for a fixed value of $n = 0.5$ 50

Table 5.3 Summary of adjustable parameters calculated at different temperatures for 1 KΩ ruthenium oxide specimen 51

CHAPTER 1

General Introduction

1.1 Introduction

Any semiconducting or insulating material is characterized by its band structure. Any deformation to the band structure and hence to the density of states (DOS), for example by doping or by enhanced intersite electron-electron and electron-impurity ion correlations, induces a rigid (Berggren and Sernelius 1985) downward shift in the conduction band. At the same time the valence band is shifted upwards. This leads to the reduction of the fundamental band-gap energy (Pantelides *et al.* 1985).

Each ion introduced into a host material creates a distinct local energy level in the band-gap. At high impurity ion densities, these local levels interact to form a band known as an impurity band. The fact that these energy states are randomly distributed in space (provided the extrinsic donor concentration is less than n_c) causes the DOS to tail into the forbidden energy gap (Kane 1985). The extent of the tail is determined by the strength of the electron - particle interactions (Van Mieghem 1992). (The particle referred to above can be an electron or impurity ion).

The history of the charge hopping mechanism in disordered systems, which poses as an alternative to the band mechanism, is traced by Shklovskii and Efros (1984). The charge hopping mechanism is of major interest in the vicinity of the metal-insulator (M-I)

transition. The exact nature of the M-I transitions, particularly in heavily doped semiconductors has been, and still is, a subject of intense theoretical and experimental investigation. Many details of the transition still remain obscure as a result of the complex *intrinsic* Coulomb correlations in the presence of the disorder. Important theoretical contributions beyond the simple band theory have been made by Mott (1974, 1990), regarding the role of the electron-electron interactions, and by Anderson (1958) on the nature of the disorder at low temperatures.

1.2 Conduction in Diamond

Diamond is considered a typical covalent solid, with neutral carbon atoms bonded to the neighbouring atoms by saturated directional bonds, which make it chemically unreactive. It is exceptionally hard and has a high coefficient of thermal conductivity - a combination that makes it an indispensable tool in the semiconductor, as well as the emerging opto-electronics industry. Diamond is thermodynamically metastable at ambient temperatures and pressures. A high kinetic activation is needed to induce the transformation to graphite. Diamonds are classified according to their impurities, which involve nitrogen atoms and associated defects. These impurity centres give rise to deep-lying energy levels within the forbidden gap and have observable effects on the properties of diamond. Such effects include an increased electrical conductivity, the appearance of electron paramagnetic resonance spectra, and pronounced optical absorption. Type IIa diamonds have a very small concentration of nitrogen centres and are classified as the purest form of natural diamond, though they still show in general, more mosaic structure (Prins 1992).

Since natural type IIa diamonds have a large band-gap (5.5 eV), intrinsic conduction takes place only at high temperatures. Above room temperature charge conduction occurs only in the presence of defects or impurities. Type IIa diamond can be changed

into a semiconductor by implantation or doping in some other way. In previous studies, an attempt was made to incorporate boron substitutionally into type IIa diamond substrate, the objective being to transform it into a semiconducting type IIb diamond. No exact results for this transformation exist yet (Prins 1992). Carbon-ion implantation into type IIa diamonds has been carried out previously by Hauser *et al.* (1976, 1977). The net implanted dose ranged from 3×10^{15} cm^{-2} to 6×10^{16} cm^{-2} and was spread over the energies, 70, 40 and 20 KeV in creating a microscopic homogeneous conducting layer of depth $\simeq$100 nm. After each implanted ion dose, they generated ohmic contacts using quick drying silver paint, and measured the resistance as a function of temperature. The measured results are shown in figure 1.1. Their data followed the Mott variable range hopping law over the whole temperature range (300 K - 20 K) except for samples far removed from the M-I transition. Hauser *et al.* (1977) concluded that the implanted ions created a number of stable graphitic (sp^2) bonds which acted as hopping centres in an impurity band. From hardness measurements, they found the layer to be still diamond-like in its mechanical properties. This issue of graphitic clusters is of a prime concern in this research report and is treated in chapter 5.

1.3 A Report on Ruthenium Oxide Thin Films

This research report also includes a study of ruthenium oxide thin film resistors, which are commercially available. RuO_2 is used primarily as a low temperature thermometer. Resistance devices made from this material exhibit the following characteristic properties: low heat capacity, fast response, predictable temperature and magnetic field dependence, fairly good thermal conductivity, excellent stability and reproducibility, as compared to carbon glass resistors (Li *et al.* 1986, Bosch *et al.* 1986). The characteristic properties of ruthenium oxide film resistors warrant these materials to be studied at low temperatures.

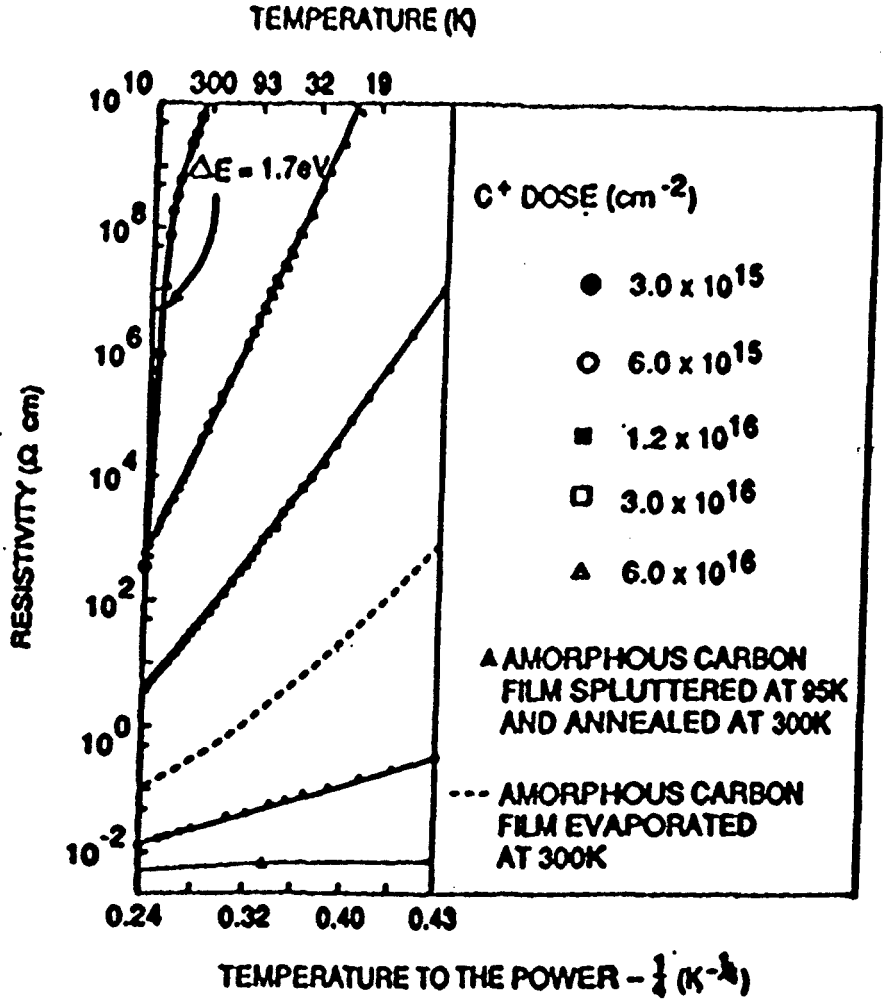


figure 1.1 Plot of $\rho(\Omega\ \mathrm{cm})$ against $T^{-1/4}$ for carbon-ion implanted type IIa diamond from 300 K to 20 K. Implantations were done at room temperature and the ion dose was spread over 70, 40 and 20 eV to effect a uniform layer of $\simeq$100 nm deep. The linearity of the curves indicates Mott's variable-range hopping conduction (Hauser *et al.* 1977).

1.4 The Scope of the Research Report

Much of the research project is concerned with systems in which electronic wavefunctions are localized in the Anderson sense. The electron hopping is strongly dependent on temperature and the impurity concentration. Because traps (bound states) are randomly distributed in position and have various energies, the conduction processes require the assistance of thermal lattice fluctuations to ensure energy conservation. The electron conduction processes were systematically studied on a carbon-ion implanted diamond surface at low temperatures.

The possible occurrence of M-I transition in heavily doped diamond samples was investigated. The effects of electron-electron interactions, which create the Coulomb gap in the one-particle density of states at the Fermi level have been examined. The Coulomb gap has dramatic effects on the variable range hopping regime and determines the form of the conductivity expression, specifically the exponent in the power law. The magnetic field effect at sufficiently low temperatures has also been studied in RuO_2 films in our investigation of magnetoresistance effects. A general observation is that, when a magnetic field is applied to a strongly disordered system, localized in the Anderson sense, the electron spins of the singly occupied states tend to align parallel to the direction of the applied field and are therefore expected to contribute to the total magnetic moment of the system. The energies corresponding to the transverse component of the **k**-wave vector are quantized into Landau levels (Nag 1980). This leads to the suppression of the hopping processes in the singly occupied states, with the net result being a decrease in electrical conduction. This effect also occurs when the electronic wavefunctions become distorted (or shrink) in the presence of a magnetic field. This reduces the overlap of the electron wave functions to the point where the electrons become localized. In this case we speak of *positive magnetoresistance*. The sign of the magnetoresistance is due to the suppression of scattering interference which causes localization, by the applied magnetic

field. Negative magnetoresistance in heavily doped (metallic) samples has been predicted by Kawabata (1980).

1.5 Outline of the Research Report

In chapter 2, the impurity conduction mechanisms observed in disordered systems are treated at length. The experimental details and sample mountings are discussed in chapter 3, while the experimental results are given in chapter 4. Chapter 5 is devoted to a discussion of the results in the light of theoretical models as applied to diamond. Finally, a short conclusion is given in chapter 6.

CHAPTER 2

Theory of Hopping Conduction in Heavily Doped Semiconductors At Low Temperatures

2.1 Introduction

Theoretical and experimental studies of steady state or direct-current conductivity in hopping electronic systems began in the 1950's (Hill and Jonscher 1979, Bottger and Bryksin 1985), with the "discovery" of impurity conduction in archetypal crystalline semiconductors such as silicon and germanium. These studies, modelled by Bloch wave theory, contributed enormously to our understanding of electronic transport processes. The basic theoretical ideas of hopping conduction, contained in a classic paper by Miller and Abrahams (1960), achieved new relevance during the past three decades with the introduction of scaling localization theories in disordered systems, with notable contributions by Ambegaokar *et al.* (1971) and Abrahams *et al.* (1979).

According to the Miller-Abrahams impurity conduction theory, thermally-assisted hopping conduction between spatially distinct localized states, which proceeds via the fixed nearest-neighbour sites, is a dominant transport mechanism in a strongly disordered system. It is governed by the tunnelling term, $e^{-2\alpha R}$, worked out from the one-band tight binding approximation model (Mott 1987) assuming hydrogenic wavefunctions (within the framework of the one-electron theory).

The transition hopping probability that describes the charge conduction in a disordered system between nearest-neighbour localized states i and j is given by the equation, derived using the Fermi Golden Rule (Miller and Abrahams 1960, Schiff 1968, Pollak and Hunt 1991),

$$P_{ij} = \gamma_{ij}\, e^{-2\alpha R} e^{-W/kT}\,, \tag{2.1}$$

where γ_{ij} is the vibrational frequency factor, which measures the strength of the electron-phonon interaction at very low temperatures, R is the energy-independent average distance between the localized impurity sites, and $e^{-W/kT}$ is the phonon term. For hopping conduction to occur, the condition $W > 2kT$ must be satisfied. (Hill and Jonscher (1979)).

2.2 Anderson Localization.

A different kind of spin localization, based on the tight binding approximation model and not dependent on electron interaction effects, was predicted by Anderson in 1958 (Anderson 1958). The disorder in the system of interest is introduced by letting the energy of the randomly and independently positioned impurity atoms vary from site to site in space. An electron moving through an array of non-identical potential wells fluctuating randomly in depths (representing the on-site energies) by more than a certain amount can be temporarily localized.

Taking the range of potential variation from $-W/2$ to $W/2$, where W is the energy of the disorder, an electron can be bound to a particular site when the ratio of W to the bandwidth (electron overlap) $B = 2zV$ exceeds a critical value, $\left(\frac{W}{B}\right)_{crit}$, with z being the coordination number. If $\left(\frac{W}{B}\right)$ is less than the critical value, then the states in the band tails are the first to become localized. (A recent review of charge hopping

in the bandtails is given by Monroe (1991) and Van Mieghem (1992)) The energies, E_c and $E_{c'}$, called the mobility edges, sharply separate the exponentially localized and the extended states (Mott 1967). The radial extension of localized wavefunctions goes to infinity as the energy approaches a mobility edge. This is schematically depicted in figure 2.1. The critical value for diamond has been calculated to be > 8 (Thouless 1978).

We now consider the situation where the electronic chemical potential (Fermi energy) μ is made to cross the mobility edge. This can be achieved by either varying the degree of disorder or the extrinsic electron density. If μ lies well above E_c (but below $E_{c'}$ in figure 2.2), the states are extended in space, and one expects a "weak scattering theory" to be appropriate in describing the electronic conduction. For $\mu < E_c$, the states at the Fermi energy are localized and the system is said to be insulating. Two forms of conduction mechanisms exist in this case: at high temperatures the charge carriers are excited above the mobility edge to the conduction band, while at low temperatures conduction is realized by the phonon-electron energy exchange mechanism. Both these processes lead to a strong temperature conductivity dependence (Mott 1987). With an increase in the disorder, E_c and $E_{c'}$ can be driven towards the band centre.

According to Mott (1967), there exits a finite "minimum metallic conductivity" decribed by the equation

$$\sigma_{\min} = C\frac{e^2}{\hbar a} \tag{2.2}$$

as μ approaches E_c (from the right in figure 2.2), where a is the interatomic spacing and C is a numerical constant. Several experiments have failed to observe $\sigma_{\min}$ (Rosenbaum *et al.* (1980) and references therein). The "deficiencies" in the concept of minimum metallic conductivity are addressed by percolation theories and other approaches (Bottger and Bryksin 1985). This idea of minimum metallic conductivity has

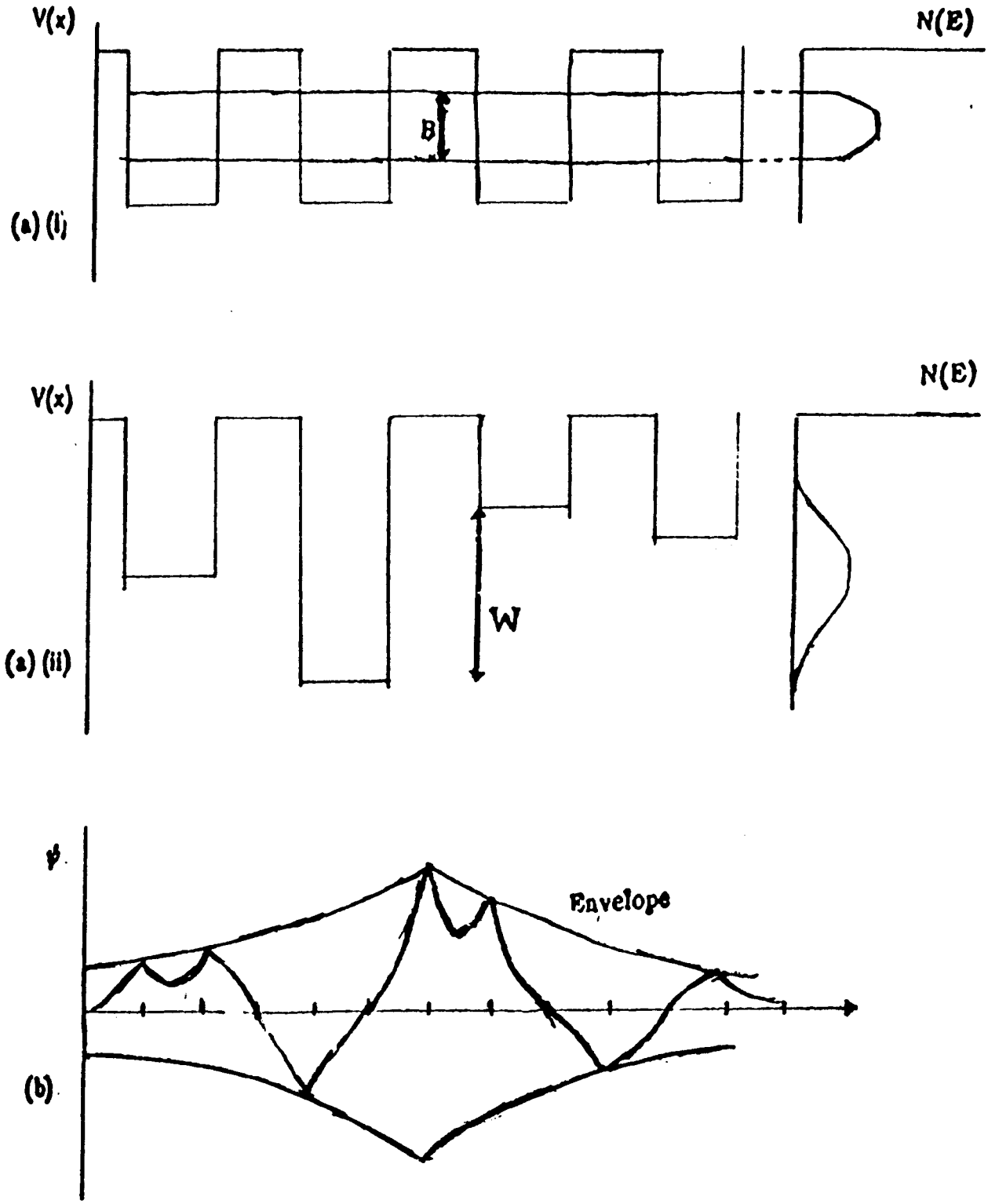


Figure 2.1 Crystalline and random potentials with the corresponding density of states. The wavefunction ψ of an electron in a weakly localized state

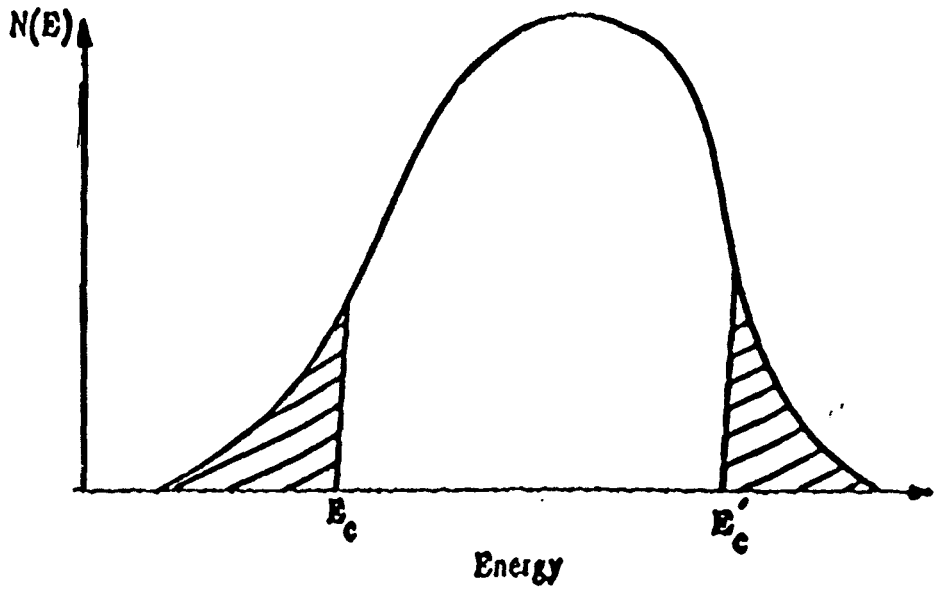


Figure 2.2 Density of states in an Anderson band with two mobility edges E_c and E_c'. The shaded states are localized.

generally fallen into disfavour, but there is still a possibility of its existence, particularly in a large magnetic field (Mott 1989, Mott and Kaveh 1985).

For a recent review on localization theory, the reader is referred to a paper by Brenzini *et al.* (1992) and references therein.

2.3 Mott and Efros-Shklovskii Conduction Theory

Mott introduced a concept of variable range hopping (VRH) conduction to address the situation where the energy for non-nearest hopping sites is a function of the spatial separation between the localized sites (Mott 1968). According to Mott, the low temperature direct-current conductivity for quasi-particles in a nonvanishing single-particle density of states (SPDOS) exhibits universal behaviour of the form:

$$\sigma(T) = \sigma_o \exp\left[-\left(\frac{T_o}{T} \right)^{\frac{1}{d+1}} \right] , \tag{2.3}$$

where T_o is the characteristic temperature, given by

$$T_o = \frac{b_d^M}{N_o a^3} \quad . \tag{2.4}$$

N_o is the density of states at the Fermi level, a is the energy-independent localization length, $d = 2, 3$ is the space dimensionality, $b_3^M = 2.2$ and $b_2^M = 13.8$.

In deriving eqn (2.3), known as the Mott $T^{-1/4}$ law, certain specific assumptions are made, which can be used as criteria for testing the applicability of VRH to the experimental data. Firstly, the DOS is taken to be a constant or slowly varying function of energy (Zhang *et al.* 1990) throughout the whole temperature range, and secondly the

electron interaction (also referred to as the electron correlation) effects is neglected. Hopping of this kind has been observed extensively in amorphous materials (Hill 1976, Hill and Jonscher 1979, Zabrodskii and Zinove'va 1984), including high temperature measurements on diamond (Prins 1992), though experimental difficulties in determining the correct exponent value in the power expression are considerable.

The Edwards-Sienko semi-log plot of effective Bohr-radius a_H^* against the critical dopant concentration n_c has buttressed and validated the Mott criterion $n_c^{1/3} a_H^* \simeq 0.25$ for most disordered systems at the M-I transition (Edwards and Sienko 1978).

Efros and Shklovskii have shown that the SPDOS in a disordered system tends to zero at the Fermi level as a result of the unscreened long-range Coulomb correlations. As a consequence, they predicted the following law using percolative arguments (Efros and Shklovskii 1975):

$$\sigma(T) = \sigma_o \exp\left[-\left(\frac{T_1}{T} \right)^{1/2} \right] , \tag{2.5}$$

where

$$T_1 = \frac{b_d^{ES} e^2}{\kappa \alpha} , \tag{2.6}$$

with $b_3^{ES} = 2.8$ and $b_2^{ES} = 6.2$.

A large part of the assembled experimental evidence for $d = 3$ disordered systems confirms the law described by eqn (2.5) (Hill *et al.* 1979, Mobius 1985).

2.4 Coulomb Gap

The importance of electron correlation effects, which lead to a soft gap in the one-electron excitation spectrum near the chemical potential, was emphasized independently by Pollak (1971) and Srinivasan (1971) in disordered localized systems. This gap has been termed the Coulomb gap (CG) by Efros and Shklovskii (1975).

Many analyses of the CG are based simply on analytical and computer simulation studies (Mott 1975a, 1975b, Pollak *et al.* 1979, Baranovskii *et al.* 1979, Davies *et al.* 1982, Levin *et al.* 1987, Mochena *et al.* 1991a, 1991b, Ortuno *et al.* 1992). The CG has been detected directly from tunnelling experiments (Wolf *et al.* 1975, McMillan *et al.* 1981), and photoemission measurements (Davies *et al.* 1986, Holinger *et al.* 1985).

No full consensus has been reached regarding the model-dependent characteristic nature of the CG and its effect on the hopping conduction (Pollak 1992). The main source of the controversy arises from the nature of the low-energy excitations. It is argued that these cannot be decomposed into short-range non-interacting and long-range interacting excitations (Pollak 1992). Efros and Shklovskii have neglected the intrasite Coulomb interactions in deriving eqn (2.5). A detailed review of the gap is given by Efros and Shklovskii (1985), Pollak and Knotek (1979), Pollak and Ortuno (1985) and Bottger and Bryksin (1985).

2.5 Demonstration of the Coulomb Gap

Consider an Anderson localized disordered system with $N-1$ electrons at $T=0$. Assume that an N^{th} electron is inserted into the system at the lowest possible energy state i, while keeping the other electrons "frozen" in their original atomic sites. The

system will be rearranged due to the electron interactions to minimize its energy in accommodating an N^{th} electron. Imagine transferring an electron from site i to site j degenerate with site i before rearrangement. The transfer is made without allowing the system to relax to a new configuration. The total energy associated with this procedure is given by

$$E_i^j = \varepsilon_j - \varepsilon_i - \frac{e^2}{\kappa r_{ij}} \quad . \tag{2.8}$$

(i.e The energy allowed for such an excitation is the difference in the single particle energies $\varepsilon_j - \varepsilon_i$, minus the interaction of the newly placed electron on the host site j with the electron on the donor site i.)

Activation energy is needed to transfer an electron from site i to site j. Part of this energy comes from the electron correlation effect during rearrangement and the other part results from the $N-1$ electrons not being in their true ground state. Since all changes incurred by the system must be real, we have that

$$\varepsilon_j - \varepsilon_i - \frac{e^2}{\kappa r_{ij}} \geq 0 \tag{2.9}$$

for all occupied sites i and empty sites j in the disordered system. Ample justification of the eqn (2.9) is given by Kurosawa and Sugimoto (1975) and Efros and Shklovskii (1985).

According to Efros and Shklovskii, the states associated with eqn (2.9) should be located as far apart as possible - one above and one below the chemical potential. The spatial density of these single-particle states, which are close in energy, is thus reduced. This effectively leads to a reduction of the SPDOS at the Fermi energy and hence the creation of the CG. The behaviour of the DOS at the Fermi level is depicted in figure (2.3).

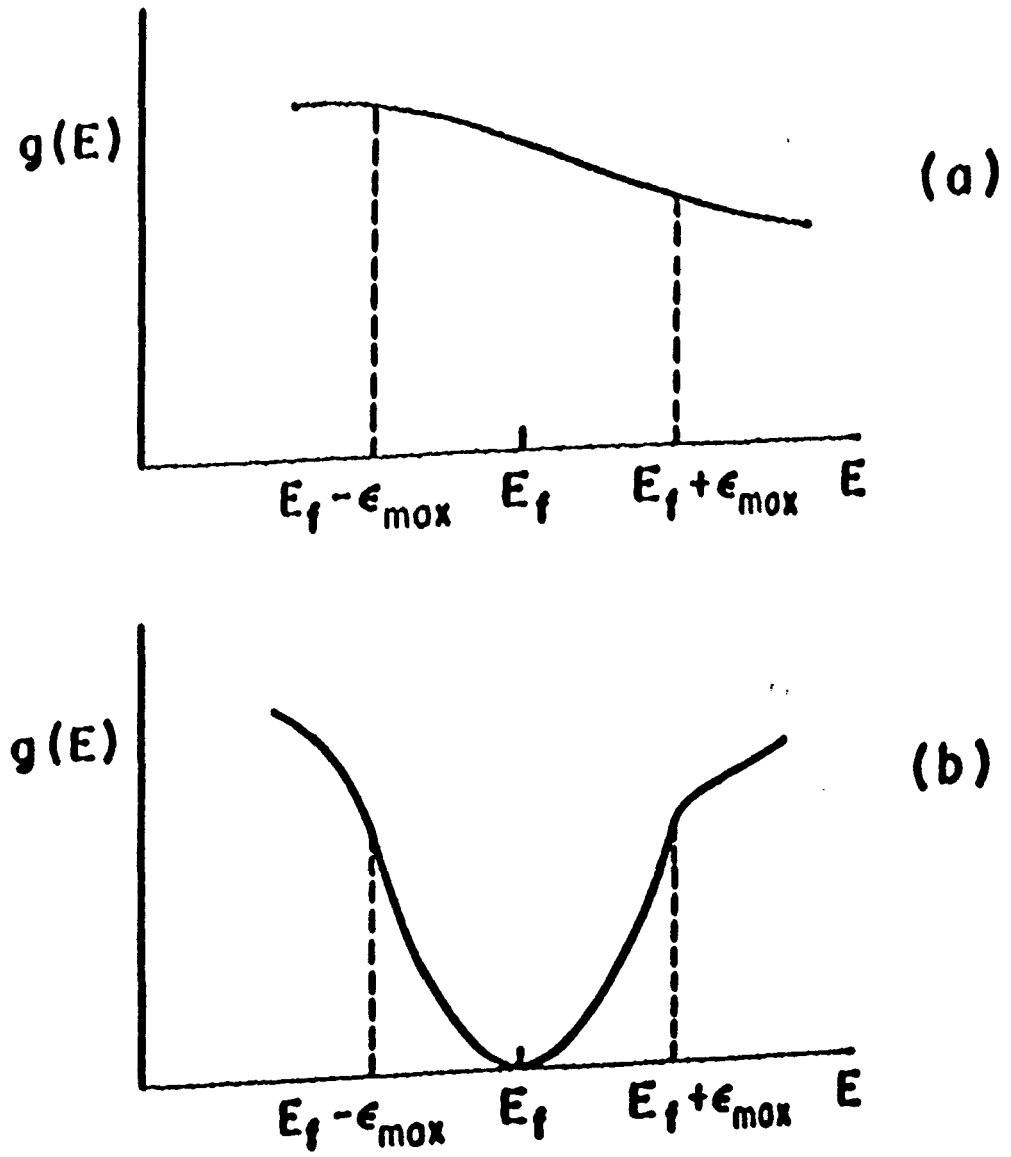


Figure 2.3 Depiction of the effect of the shape of the density of states, $g(E)$, on the number of states near the Fermi energy. (a) $g(E_F) \neq 0$, (b) $g(E_F) \propto | E - E_F |^2$.

2.6 Effect of the Coulomb Gap in the VRH regime

The dramatic effect of the CG in the VRH conduction regime has been observed in low temperature measurements. The effect manifests itself more strongly with the switch-over from Efros-Shklovskii hopping to Mott hopping behaviour. A stronger than parabolic decrease in the SPDOS for the divergence of the CG for smaller $\tilde{E} = E - E_F$ has been derived by several authors, based on the many-body electron transitions and electron-phonon coupling theory (Chicon *et al.* 1988, Castner 1991).

Closely associated with a cross-over from Efros and Shklovskii conductivity to Mott's law are the occurrence of shallower gaps, known as "hard gaps", which resemble those of the soft CG observed in ordered systems. The SPDOS in this case depends exponentially on E (Voegele *et al.* 1985, Vinzelberg *et al.* 1992). The concept of conductivity cross-over is mentioned in chapter 5. The most obvious explanation for a cross-over is a closure of the CG due to the divergence of the low frequency relative permittivity as the sample conduction changes (Castner 1991).

CHAPTER 3

Experimental Details

3.1 General Considerations

Ion implantation is a physical mechanism in which *foreign* atoms (or ions) are introduced into the host material by bombardment. Implantation is usually carried out with the substrate at very low temperatures, typically of the order of liquid nitrogen temperature. Use of the implantation technique affords the possibility of introducing a wide range of atomic species into the substrate, thus making it feasible to obtain the dopant impurity concentrations, energy and positional distribution of interest. Some of the major factors governing ion implantation are the amount and nature of the lattice disorder created, the range distribution and the location of the implanted atoms within the crystal's unit cell, electrical characteristics resulting from the implantation and the subsequent annealing treatments. These factors are discussed in papers by Prins (1985, 1988a, 1988b, 1989, 1991), and only a brief discussion will therefore be given.

3.2 Lattice Disorder

An implanted atom always creates radiation damage when it thermalizes into the host material. It displaces other atoms from their lattice sites which, in turn, may displace other atoms as they cascade (*i.e* undergo secondary collisions processes), depending on

the energy of the incident atom, with the net result being the production of a highly disordered region around the path of the incident atom, most prevalent at the end of the ion's track (Ryssel *et al.* 1986). The retardation of ions in the substrate material has been termed *nuclear stopping* and is detailed in many publications. The lattice damage incurred during implantation is usually annealed out at preselected higher temperatures.

3.3 Range Distribution of the Implanted Atoms

Much effort has been directed at experimental and theoretical work leading to a clear-cut understanding of the energy loss processes that govern the range distribution of implanted atoms (Derry 1980, Spitz 1990, Mayer *et al.* 1970). Most of the factors influencing ion implantation, for example a typical range distribution in an amorphous substrate, can now be predicted. From the energy loss mechanism the nature of the lattice disorder produced during implantation can be determined and the *depth profile* as a function of accelerating voltage of the implanted dopant atoms can be controlled.

The range distribution depends strongly on the orientation of the crystal axis or plane, *i.e* the channelling effect. If an ion impinges on a crystal almost parallel to a major axis, in the case of diamond $< 110 >$, then a correlated series of collisions may steer it gently through the crystal 'channel', thus reducing its rate of energy loss and increasing its penetration depth. Figure 3.1 shows an axial orientation of $< 110 >$ in a diamond type lattice and a 'random' direction at $\simeq 10°$ from $< 110 >$. In figure 3.1(b), a typical uniformly disordered system, as expected after implantation, is shown.

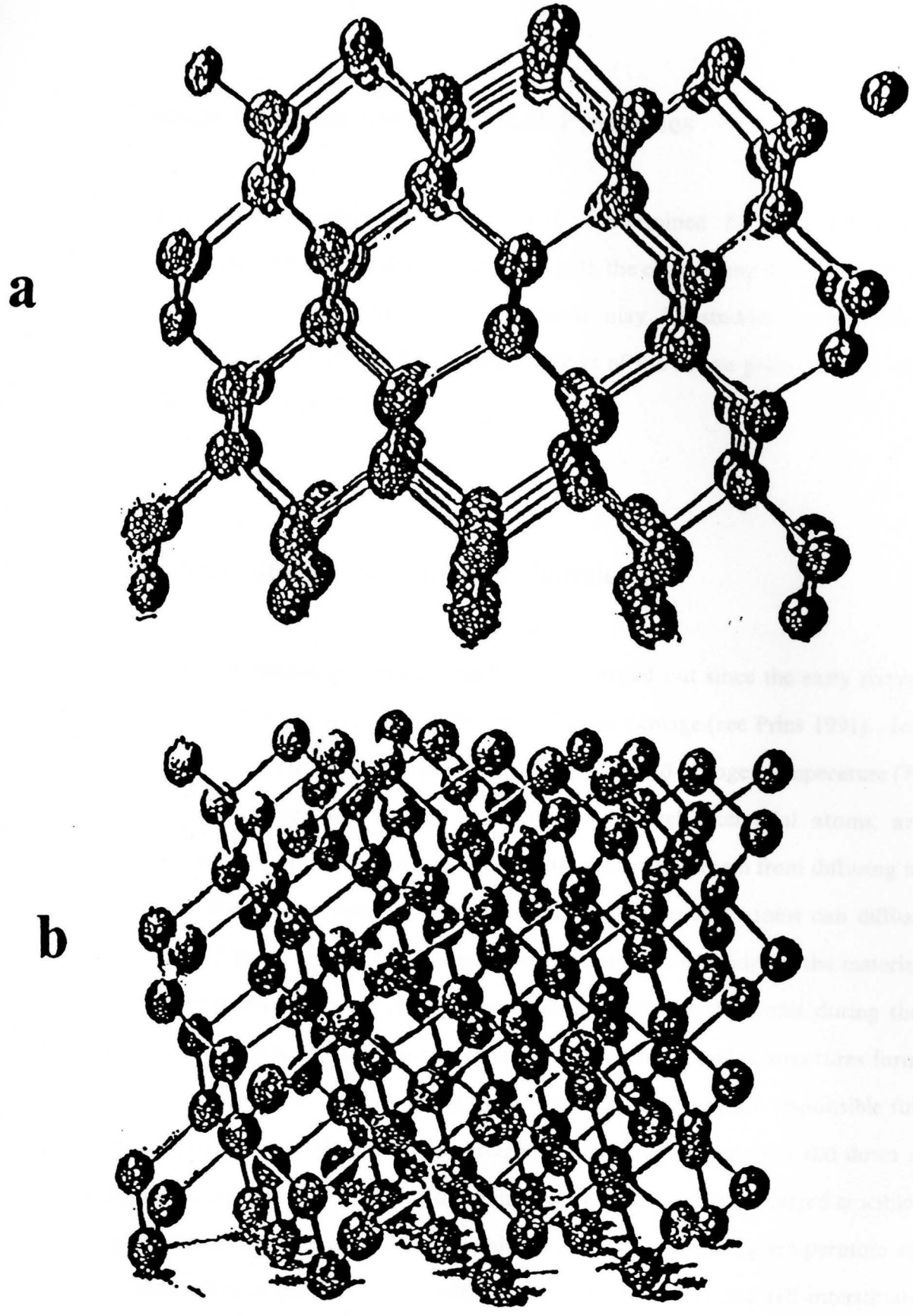


Figure 3.1 Diamond type structure showing (a) < 100 > axial orientation and b) 'random' direction at 10° from < 110 > (Mayer *et al.* 1970).

3.4 Lattice Location and Electrical Properties

The location of the implanted atoms can be determined by the Rutherford backscattering (RBS) process used in conjunction with the channelling process (Sawicka *et al.* 1981). The electrical conductivity behaviour may be studied by Hall-effect measurements (Vavilov *et al.* 1970). Detailed reviews of the above properties are also covered in Mayer *et al.* (1970).

3.5 Ion Implantation in Diamond Samples

Diamond doping by means of implantation has been carried out since the early sixties, with some earlier claims to success ascribed to radiation damage (see Prins 1991). Ion implantation is carried out at low temperatures, typically liquid nitrogen temperature (77 K). At this temperature, defects such as vacancies and self-interstitial atoms, are effectively 'frozen' in their occupational positions, thus impeding them from diffusing in the substrate. Well above room temperature some self-interstitial atoms can diffuse from an implanted layer, leaving behind an excess of vacancies, which lower the material density, thus promoting the formation of complex agglomerate structures during the annealing cycle and possibly leading to graphitization. These complex structures form deep-lying donor centres at $\simeq$4 eV below the conduction band and are responsible for the electrical properties of the material. After implantation, the sample is slid down a chimney in an argon gas atmosphere with minimum time delay into a preheated crucible. Argon gas is used to prevent possible graphitization at the annealing temperature of 1200°C. Annealing is performed for half an hour. At this stage the self-interstitials introduced during implantation are detrapped and diffuse through the material, recombining with the vacancies and thus reducing the lattice damage incurred during implantation. The dopant substitutional atoms also combine with some of the vacancies

and are believed to be optically active, acting as donors (Prins 1989, 1991). It is suggested that the residual vacancies group together and form a structure which has been termed a *vacloid* (Prins 1992). The issue of vacloids is still delicate at this stage and is treated with restraint in chapter 5.

3.6 Sample Preparation

Polished rectangular and insulating type IIa diamond samples were obtained from the De Beers Diamond Research Laboratory. Polishing of the samples depends on the axial orientation. From the cubic symmetric nature of the diamond samples, it is observed that $< 100 >$ has four polishing directions and $< 110 >$ has two. These surfaces are known in the diamond industry as four-pointers and two-pointers respectively. The directional plane $< 111 >$ is regarded as *extremely* difficult to polish and to prepare. Cutting diamonds by laser has now become popular in industry. Difficult planes can be prepared using this technique (Prins 1992). Due to metastability of diamond, the preparation technique may leave graphitic-type materials (which can be difficult to remove) on the surface which can conduct electrically. This can lead to erroneous conductivities being measured when attempting to dope diamond selectively by means of ion implantation.

It has been previously observed that *any implanted species* , including inert atoms such as argon and xenon (Vavilov 1975), can create a conductive surface layer in diamond. This can only imply that the resultant radiation damage is electrically active. Cases have been reported where the virgin electrical resistance of the diamond samples was incredibly low. The cause of this in most cases has been the termination of carbon dangling bonds on the surface by hydroxyl radicals (Vandersande 1976, Derry *et al.* 1983). With this background knowledge, carbon-ion implantation has been carried out

with great care (Prins 1991) to create a fairly uniformly disordered conductive surface in diamond samples. The depth of the implanted layer from the surface is about 1000 nm and can be determined using the standard TRIM 89 (Spitz 1990) Monte-carlo computer simulation program. A build up to the total ion dose for the implanted sample, 5.65×10^{15} cm^2, with accelerating energy is shown in table 3.1. The values of the ion doses are determined from TRIM 89. Henceforth, we shall classify the samples according to their implanted doses- 5.65×10^{15} cm^{-2} (strong hopper), 5.70×10^{15} cm^{-2} (mild hopper) and 5.85×10^{15} cm^{-2} (weak hopper). The table shows the range of energies and implantation doses used in preparing one of the samples (strong hopper).

Energy (KeV)	Implantation Dose ($\times 10^{15}$ cm^{-2})
150	2.260
120	1.469
80	1.243
50	0.678
	total implant: 5.650×10^{15} cm^{-2}

Table 3.1 Energies at which carbon ions were accelerated into the diamond at nitrogen temperatures. The values of ion doses are determined from the TRIM 89 computer program.

3.7 Sample Cleaning

After the implantation and annealing cycles, the samples were cleaned by boiling them in a solution of perchloric, nitric and sulphuric acid to remove *shadowing* from their sides and to dissolve graphite and amorphous carbon layers formed during implantation. The solution was placed in a small beaker, covered with a glass plate and heated under constant temperature until it turned yellowish in colour. The beaker (with samples inside) was cooled by putting it in cold water. The samples were then rinsed in distilled water.

Alternatively, the samples, placed in a beaker, were cleaned in an ultrasonic bath using the solvents below in the listed order shown, with each run lasting at least 5 minutes:

(i) Trichloroethylene
(ii) Methanol
(iii) Acetone
(iv) Methanol
(v) Acetic acid
(vi) Distilled water
(vii) Propanol

The samples were then immediately flushed with nitrogen gas to let the propanol evaporate.

3.8 Sample Mounting

Samples were placed on a specifically designed sample holder made up of a bottom brass plate, (later replaced by a steel plate), with a recess to accommodate the diamond

sample, a top steel plate glued to a perspex sheet, and electrical copper contacts. Four grooves were made in the perspex sheet, in which the contacts were fitted.

The perspex sheet was stuck to the metal plate and the attached electrical contacts were thoroughly cleaned in the detergent solution, rinsed in distilled water and then in alcohol, before the sample was mounted on the holder. A schematic view of the sample holder is shown in figure 3.2.

3.9 Electrical Contacts

A four-point probe contact resistance technique was used to measure the sample resistances. Annealed copper wires of diameter 0.65 mm were used. These copper wires were found to behave non-linearly with temperature for samples far removed from the transition. For two-point probe measurements, the diamond samples were sputtered with gold at the ends (edges). The copper contacts were mounted on the gold strips with quick drying thermal contact silver (epoxy) paint and then baked in a furnace at 160°C for 2 hours. The objective was to measure the sheet resistance (square resistance) at room and nitrogen temperatures, compare it with the values obtained with copper two-point probe measurements and ultimately link our results with high temperature measurements made by Prins (1992)[1] (chapter 4).

---

[1] The results are unpublished.

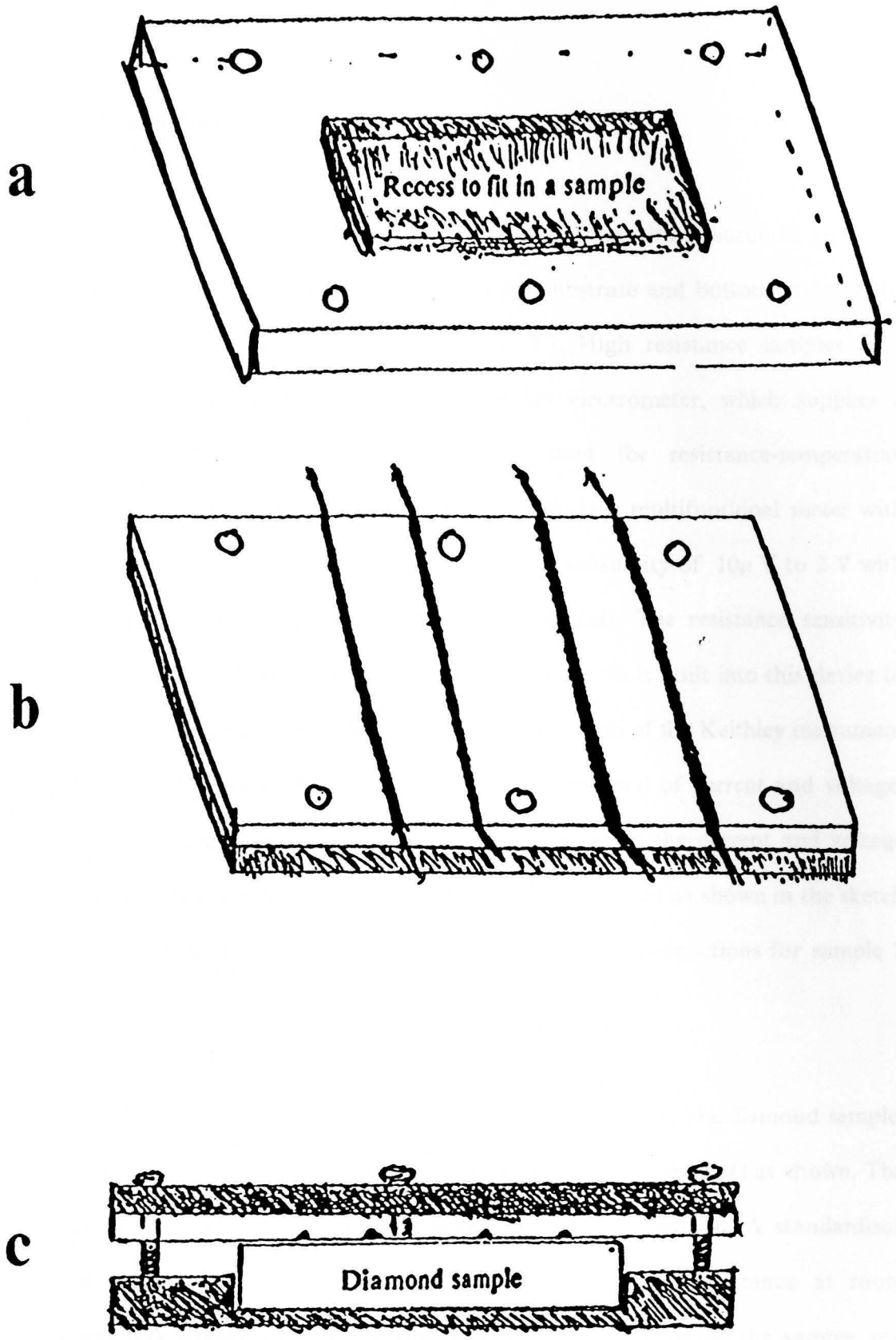


Figure 3.2 Sample holder used to mount diamond samples

3.10 Measuring Procedure

The samples were mounted on a copper substrate in a probe with Apiezon M grease to provide a good thermal contact between the copper substrate and bottom plate of the sample holder. The probe is sketched in figure 3.3. High resistance samples were mounted on the position marked 1 and a Keithley electrometer, which supplies a standardised current through the sample, was used for resistance-temperature measurements. The Keithley Electrometer (model 614) is a multifuntional meter with an in-built current sensitivity of 10^{-14} A and a voltage sensitivity of 10μ V to 2 V with an input impedance of greater than $5.0 \times 10^{13}\ \Omega$ (50 TΩ). The resistance sensitivity ranges from 1 Ω to 200 GΩ. A special preamplifier circuit is built into this device to give it the electrometer characteristics. A detailed description of the Keithley instrument is given elsewhere (White 1988). The leads from the probe end of current and voltage, (represented in bold in figure 3.3), were directly connected to the current and voltage contacts. The other current and voltage contacts were connected as shown in the sketch 3.3. This is known as a four-point probe measurement. The connections for sample 2 are shown.

Figure 3.4 shows the *'naked view'* of the copper contacts resting on the diamond sample, with the effective sample resistances denoted by $R_1(T)$, $R_2(T)$ and $R_3(T)$ as shown. The resistances of the copper contacts are denoted by r_1, r_2, r_3 and r_4. A standardised current of 9.993 μA or 100 pA (depending on the sample resistance at room temperature) was passed through the current copper contacts across the sample and back. Both direct and reversed current were used since a sample can exhibit different surface characteristics. To serve as further insulation to the samples from the copper probe-cover and to keep them in position, samples were wrapped with teflon tape.

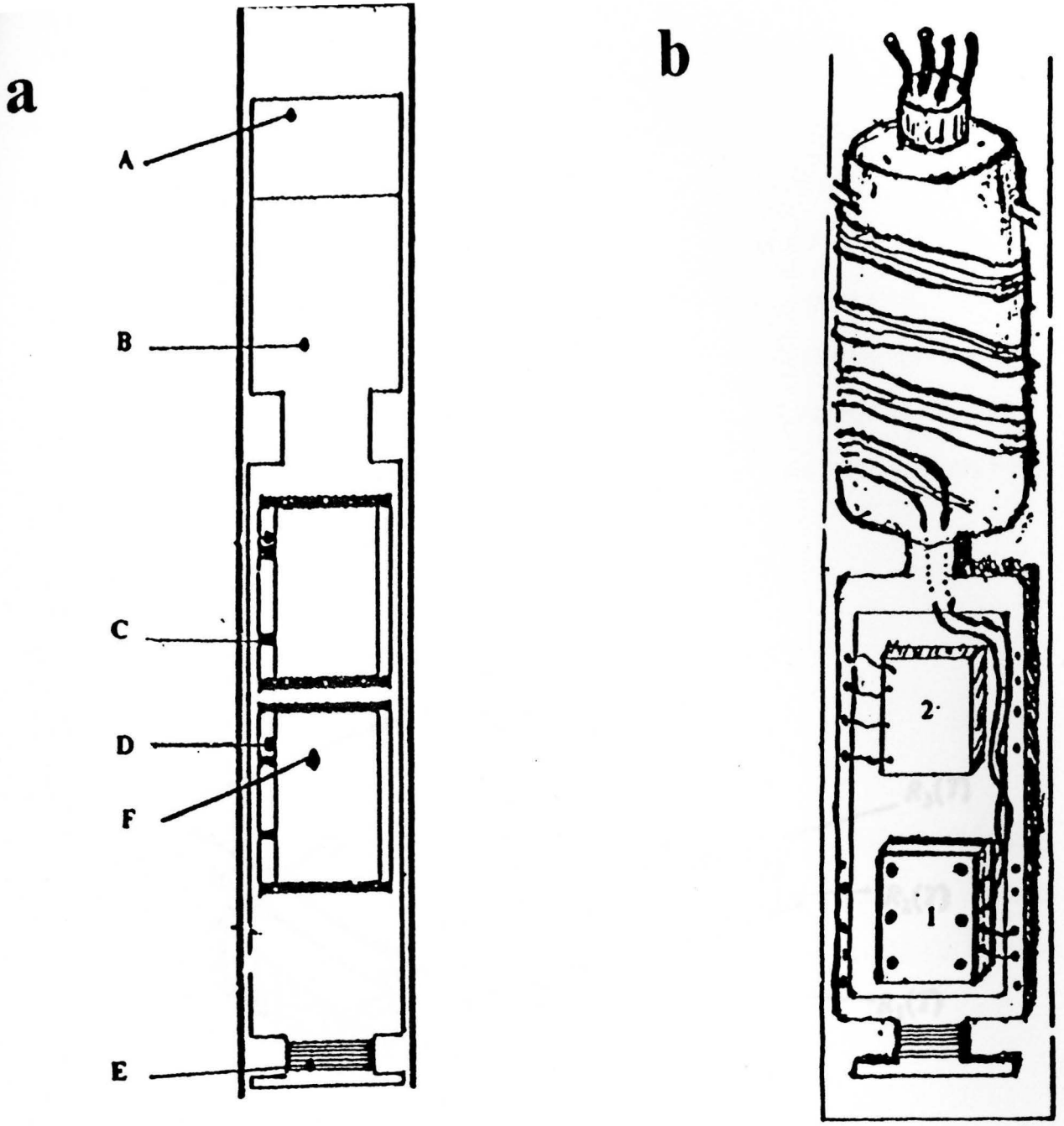


Figure 3.3 Dip stick used for sample mounting. A: Attachment to stainless steel tube. B: Copper block. C: Copper voltage contact. D: Bottom sample holder. E: Heater for temperature control (not used). F: Rh/Fe thermometer for temperature measurement (mounted at the opposite end of the copper block).

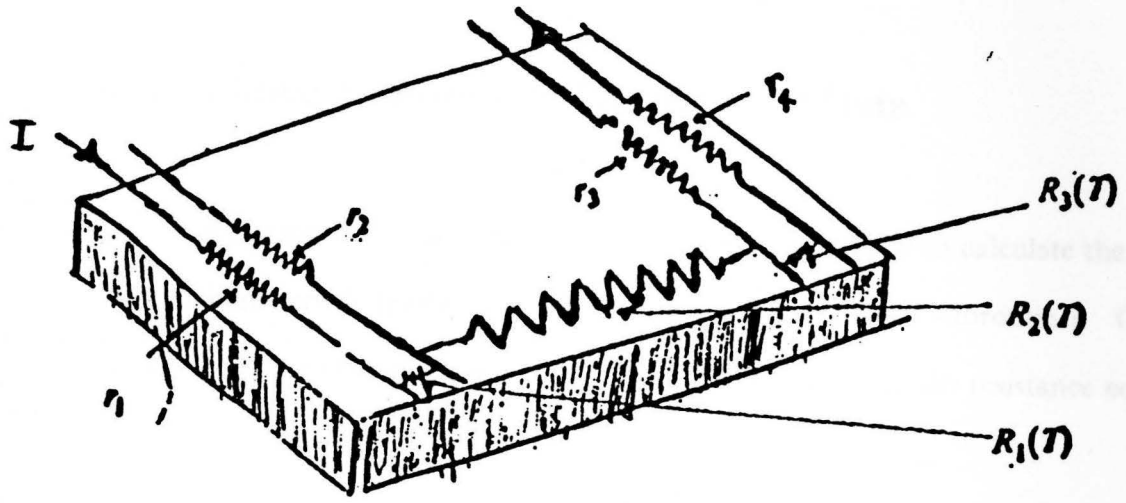


Figure 3.4 Schematic view of copper contact pressed on diamond sample.

A vacuum was created and helium exchange gas introduced into the probe cover, in order to prevent air moisture (dampening) on the samples and to maintain the same temperatures (equilibrium with the system as a whole). The probe was then mounted on the liquid helium IV cryostat. Measurements were made by dipping a probe stick slowly into a dewar filled with liquid helium. A Rhodium-Iron (Rh/Fe) thermometer was used to measure the temperatures per one degree change for a fractional resistance value measured between the voltage contacts. The measurements were made until the boiling point of liquid helium (4.2 K) was reached.

3.11 Fitting Procedure to Experimental Data

Computer programs (attached in the appendix) were developed to calculate the slope n and the characteristic temperature T_o, using the IMSL / CMS subroutines. Of major importance is the determination of the value of the index n in the resistance equation,

$$R = R_o \exp\left[\left(\frac{T_o}{T}\right)^n\right]. \tag{3.1}$$

This n value determines the form and the nature of charge conduction and depends on the physical behaviour of the DOS at the Fermi level. The method used to determine the value of n is outlined below.

3.11 (a) *Spline-curve Fitting Method*

The activation energy, $W_o(T)$, at a particular temperature was determined from the equation proposed by Zabrodskii (1977) as

$$W_\sigma(T) = -\frac{1}{T}\frac{\partial \ln \sigma}{\partial \frac{1}{T}} \quad , \tag{3.2}$$

where σ is the electrical conductivity. The eqn (3.2) can be written conveniently as

$$W_\sigma(T) = -\frac{\partial \ln R}{\partial \ln T} \simeq -\overline{T}\frac{\Delta \ln R}{\Delta T} \quad . \tag{3.3}$$

Substituting (3.1) into (3.3) gives

$$W_\sigma(T) = -n\, T_o^n\, T^{-n} \quad . \tag{3.4}$$

Therefore,

$$\log W_\sigma(T) = -n \log T + \log(n\, T_o^n) \quad . \tag{3.5}$$

Despite the fluctuations in the experimental data, due to noise as shown in figure 3.5 (a), particularly for high temperature measurements, the points tend to lie in a straight line with a slope of $-n$ and a y-intercept of $\log(nT_o^n)$. R_o can then be determined by substituting the values of n and T_o in eqn (3.1).

A second procedure follows from equation (3.3). A spline equation was fitted per four successive points to calculate the logarithmic gradient n. This method is covered in many standard computer textbooks (Vetterling *et al.* 1988 and references therein) and papers (Zabrodskii 1981, Zabrodskii *et al.* 1984). Plots of $\frac{\partial \ln g}{\partial \ln T}$ against $\ln g$, where $g = 1/R$ is the conductance, (figure 3.5(b)) allowed us to identify the ranges of the conductivity and temperature over which equation (3.1) is obeyed. To give an appropriate weighting to the measurements, we either allowed all the parameters to vary or imposed a condition, $n = 1/2$ or $n = 1.0$, to obtain the best corresponding value of R_o and T_o. It must be emphasized that fitting to limited data with three adjustable parameters determines these parameters with low precision.

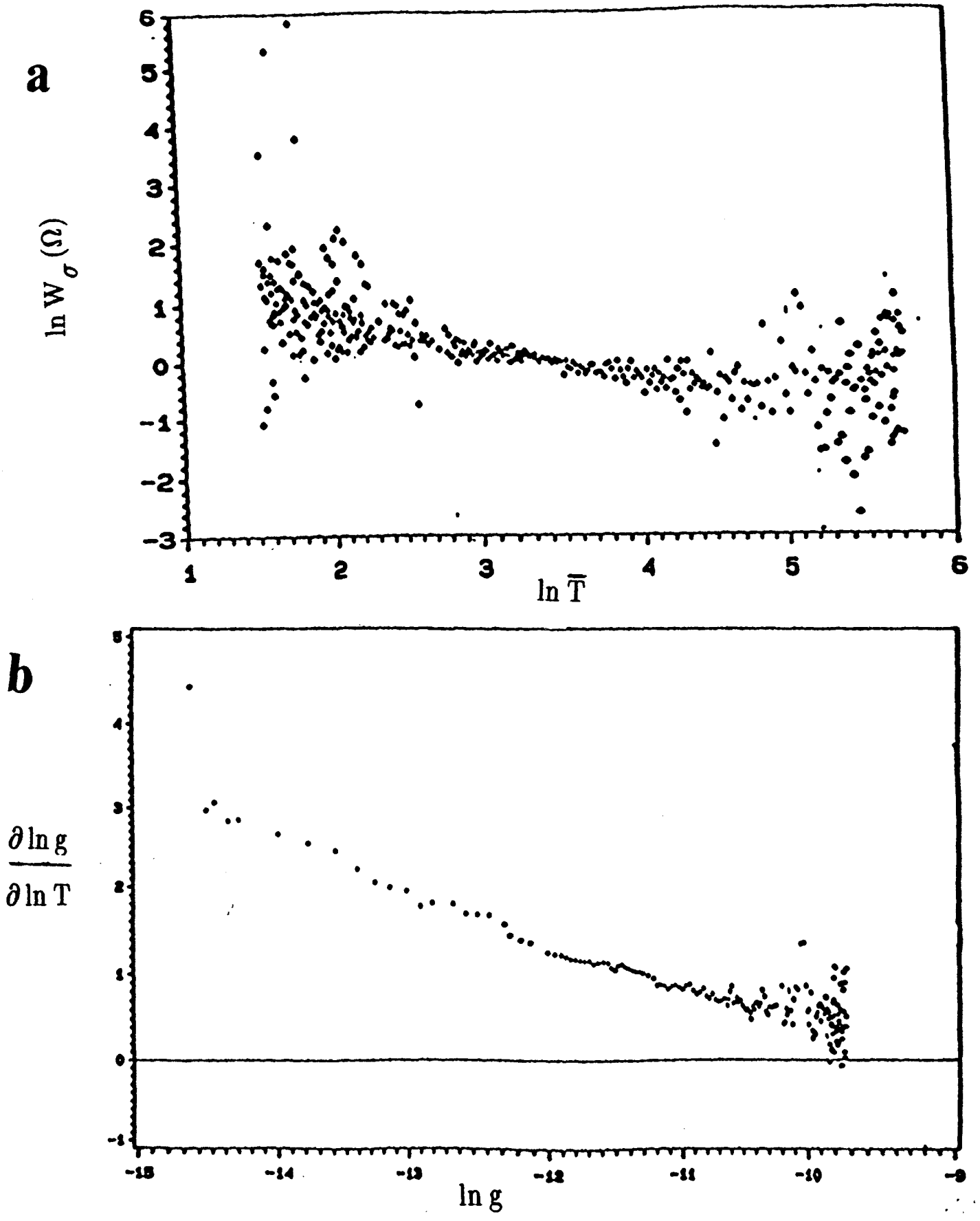


Figure 3.5 (a) Plot of ln $W_{\sigma}(\Omega)$ against ln $\overline{T}$ for a mild hopper. Measurements were obtained using four point probe resistance measuring technique. Similar plot of this kind was obtained for a strong hopper.

(b) Plot of $\frac{\partial \ln g}{\partial \ln T}$ against $\ln g$ where $g = \frac{1}{R}$ is a conductance in units of $\frac{h}{2e}$. The data was analysed using a Minuit fit computer program attached at the appendix. The data shown are for a mild hopper

The deviation in the calculations of T_o and R_o from the theoretical curve were also determined from the equation

$$\chi^2 = \sum_{i=1}^{n} (\log R_{expt} - \log R_{theor})^2 \ . \tag{3.6}$$

As a further procedure, we transformed eqn (3.1) into the form

$$\log R = \left(\frac{T_o}{T} \right)^n + \log R_o \ , \tag{3.7}$$

in order to test the data sets for known forms of hopping conduction. To make a comparison with the Mott and Efros-Shklovskii laws, plots of the dependences, $\log R$ against $T^{-1/4}$ and $T^{-1/2}$, were made to check how close the experimental data were to a straight line. This method was found to be the most convenient and has been used to analyze the data.

CHAPTER 4

Experimental Results

In this chapter the results obtained for the temperature characteristic studies on carbon-ion implanted type IIa diamonds and ruthenium oxide thin films are presented. Four- and two-point contact resistance measurements were made using the annealed copper wires and sputtered gold contacts, as described in chapter 3. We report largely on the four-point probe resistance measurements, since we found them to be the most trustworthy (Williams *et al.* 1970).

4.1 Diamond Results

The raw data for carbon-ion implanted type IIa diamond samples consist of measurements of resistance as a function of temperature. Temperatures ranged from 4.2 K to 290 K. The resistance, and hence the conductivity, was found to be extremely sensitive to the ion dose, particularly at very low temperatures. Figure 4.1 shows a semi-log plot of temperature-dependent sheet resistance for the three diamond samples measured at 290 K, 100 K and 50 K. The resistance drops very sharply as a result of the rapid decrease in the activation energy (traditionally denoted by ε_3 (Pollak *et al.* 1985)) with increasing ion dose. The magnitude of the drop increases steeply as the temperature of the resistance measurements is lowered as can be seen from figure 4.1. An increase in the carbon-ion doping level enhances the overlap of the wavefunctions of the neighbouring centres and leads to a smaller ε_3, as shown in the curve marked 3 from

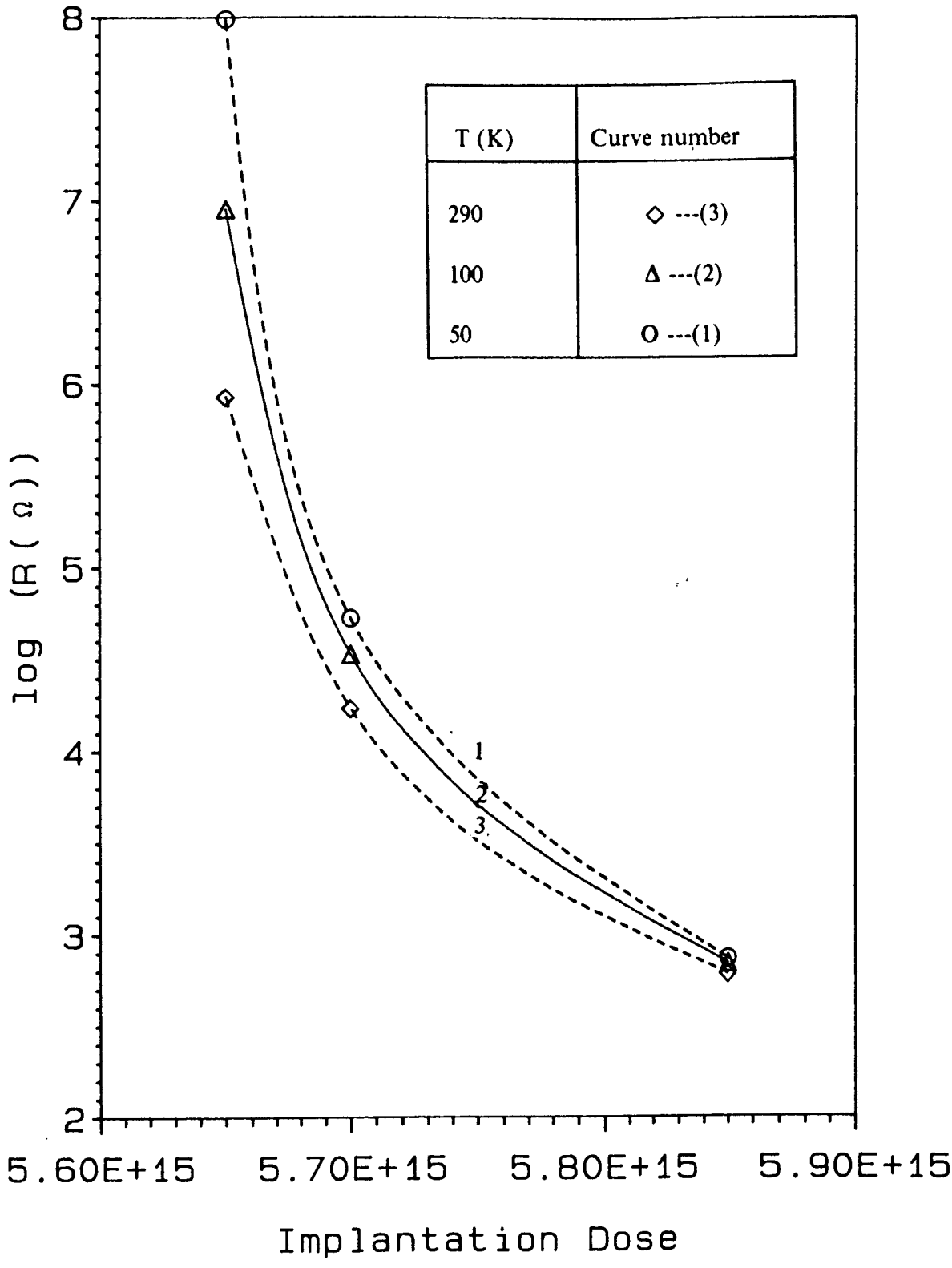


figure 4.1 Plot of log (Res (Ω)) against implantation dose for the diamond samples used at different temperatures. The four-point probe measuring technique was used to take measurements. The inset picture shows the temperature and curve number.

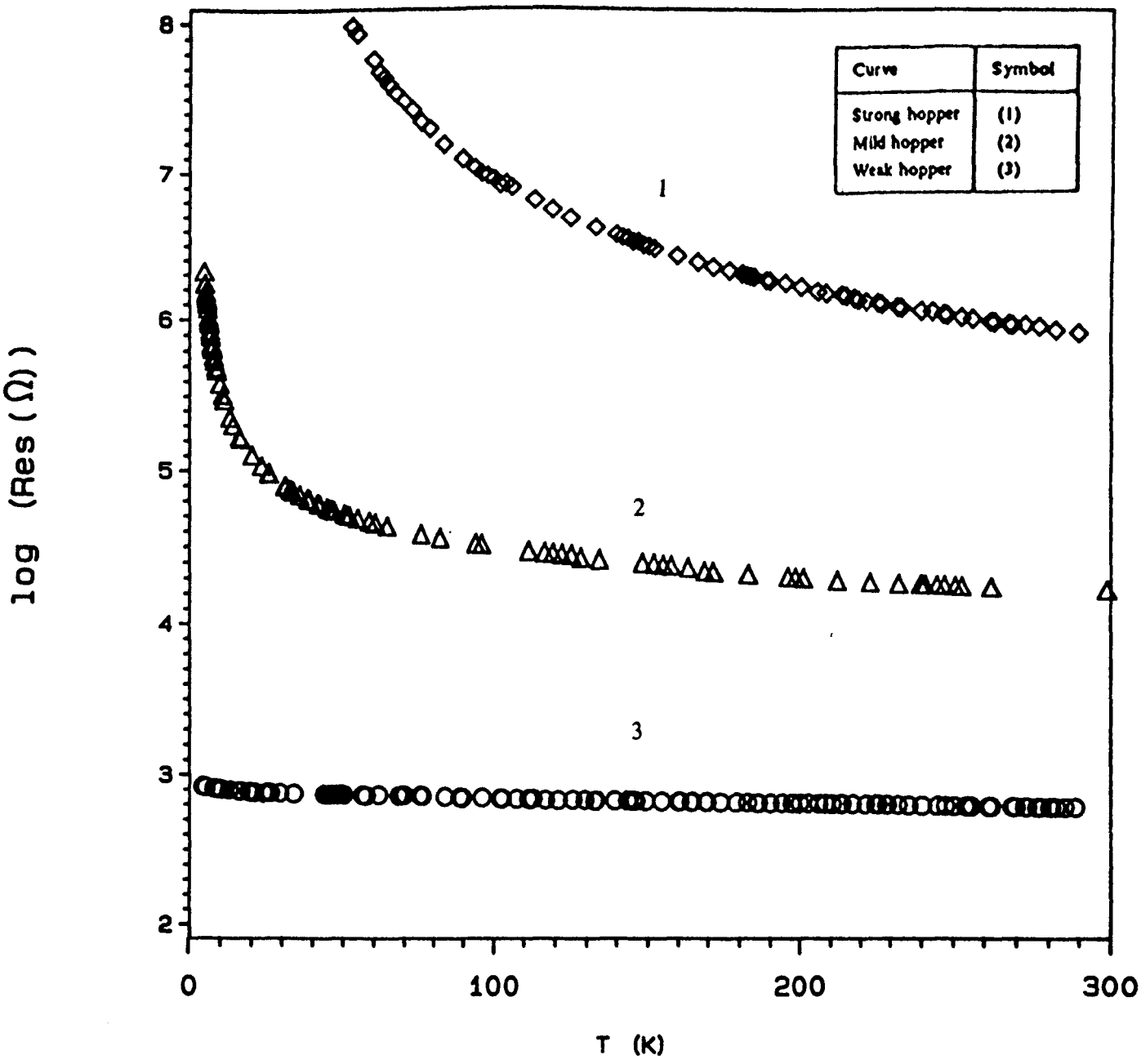


figure 4.2 Plot of log (Res) against T (K) for diamond samples.

figure 4.2. The activation energy vanishes at $N_{C+} = 5.85 \times 10^{15}$ cm^{-2}, which means that the charge conduction process for this sample has been studied in the vicinity of the M-I transition (of Anderson type), from the insulating side. The electron transport mechanism in doped semiconductors and disordered systems is governed by different conduction processes. Several of these transport processes are distinguishable in figures 4.3 - 4.5, which reflect the temperature-dependent resistance measurements for different n values. Of interest are the graphs of $\log R$ against $T^{-1/4}$ and $T^{-1/2}$. From figures 4.4 - 4.5, it is observed that in the dilute limit far away from the transition, conduction takes place in the conduction band with an activation of ε_1 at higher temperatures, and by phonon-assisted hopping between neutral and ionized donor centres at low temperatures.

4.2 Results of Two-point Probe Contacts

The fundamental aim of the experiment was to establish some link with measurements made at high temperatures on the *same* samples (Prins 1992)[2] in which Mott hopping behaviour was observed. Both plots of $\log R$ against $T^{-1/4}$ and $T^{-1/2}$ tend to follow straight lines, making it difficult to establish the true form of conduction. Another point of concern was that the sample used for this experimental run broke into several parts. Fortunately this happened after the four point probe resistance measurements were made. A large piece selected for the two-point measurements had a deep crack, which could have affected the characteristic properties of the sample, particularly after the baking of the contacts in the furnace, as described in chapter 3. We observed a slight

---

2 These results are unpublished. The previous published results, though for different implantation doses, show Mott's VRH behaviour at high temperatures (Prins 1991). Charge hopping conduction occurs through the vacloids centres.

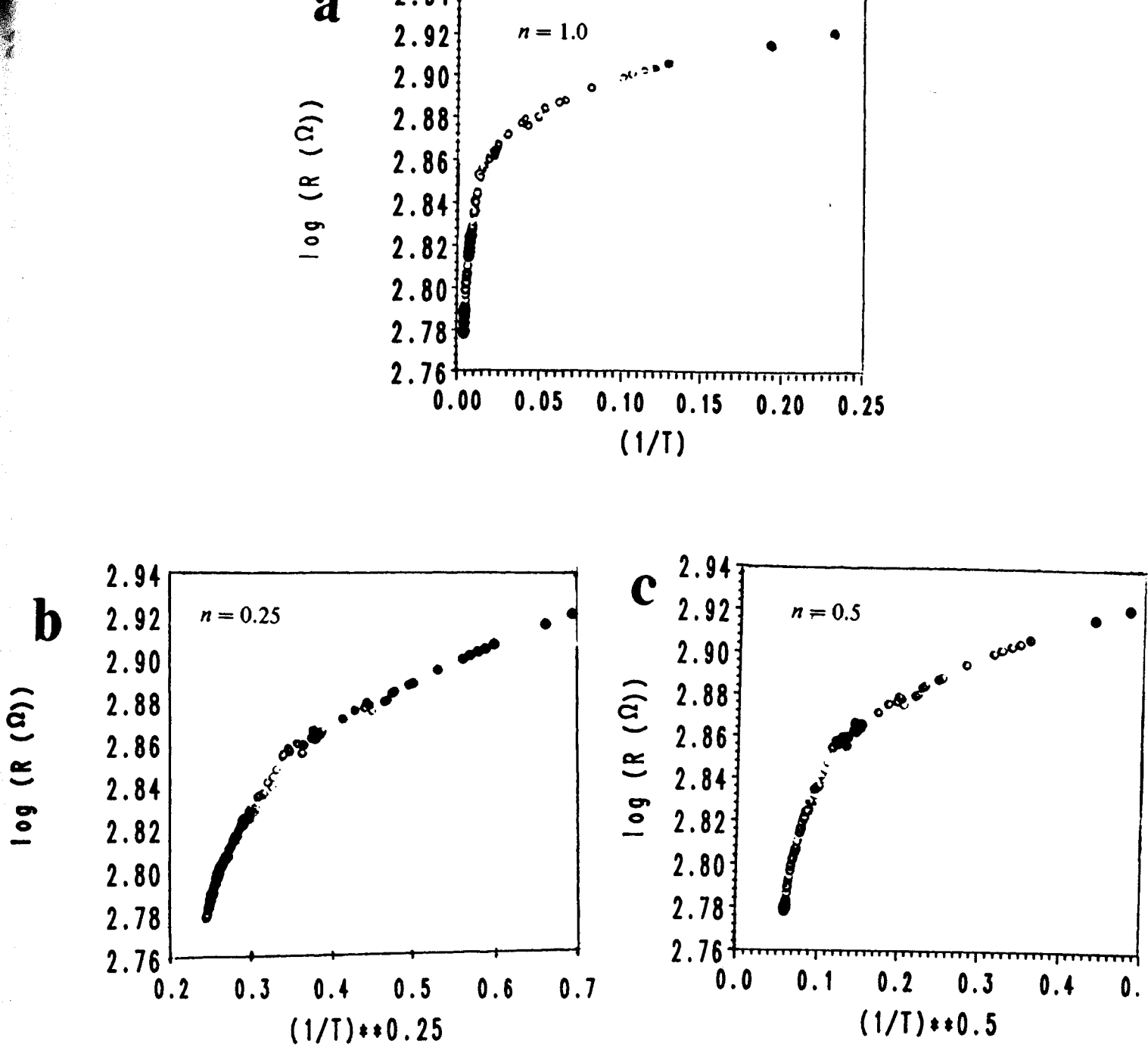


Figure 4.3 Plot of log $R(\Omega)$ vs $T^{-n}(K^{-n})$ for a weak hopper. Measurements were made using the four lead measuring technique.

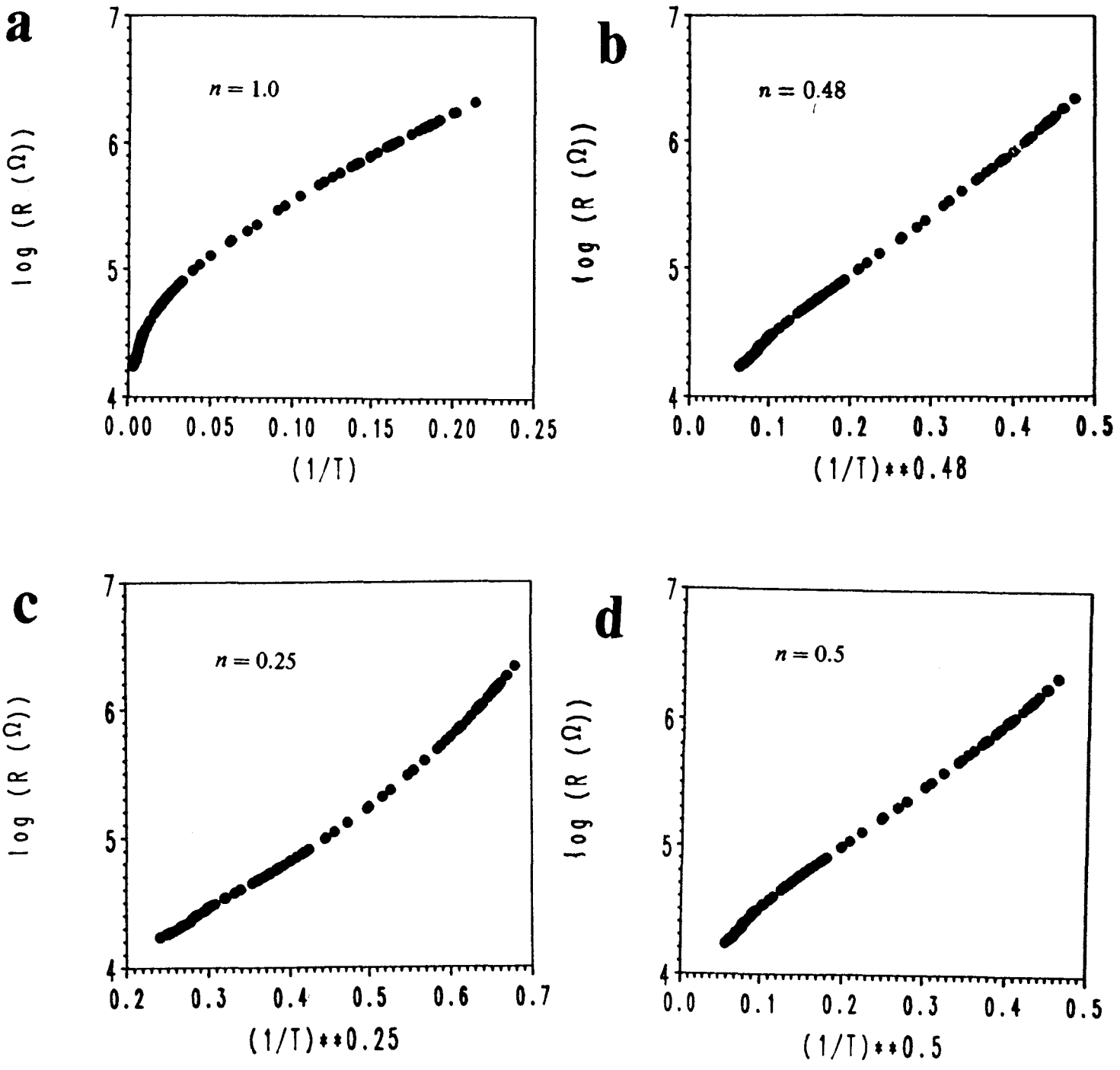


Figure 4.4 Plot of log $R(\Omega)$ vs $T^{-n}(K^{-n})$ for a mild hopper. Measurements were made using the four lead measuring technique.

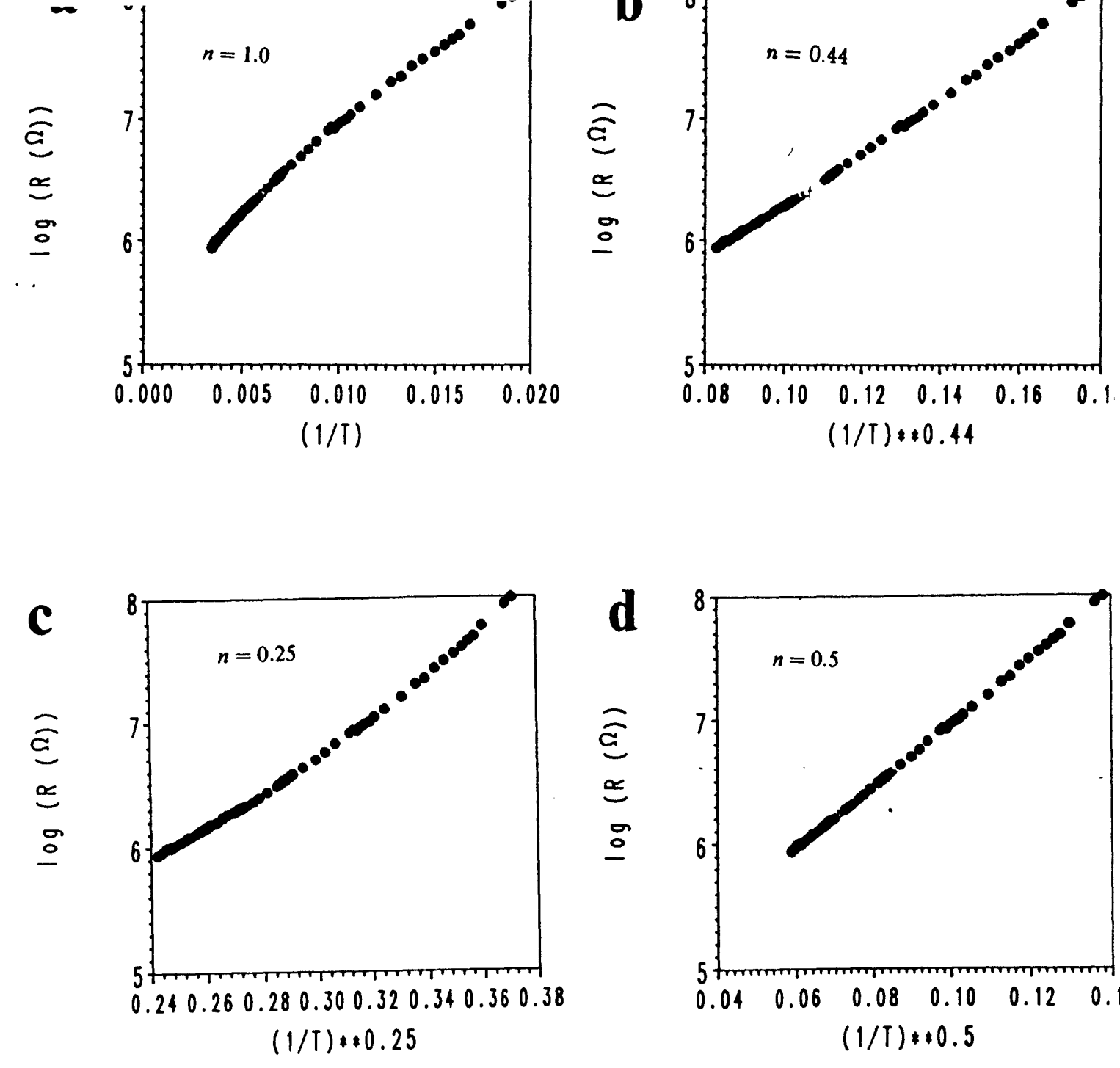


Figure 4. 5 Plot of log $R(\Omega)$ vs $T^{-n}(K^{-n})$ for a strong hopper. Measurements were made using the four lead measuring technique.

decrease in the resistance of this sample at room temperature when compared to that of the whole sample.

Different resistance measuring devices, *viz* a Fluke (Multimeter) and a Keithley model 614 electrometer, were employed to measure resistances at room temperature and nitrogen temperature. The measurements are shown in figure 4.6.

4.3 Results of RuO_2 Thin Films

Two thin films of RuO_2 of 1 KΩ and 30 KΩ with resistances at room temperature were studied using the 4-lead measuring technique. After a series of experimental runs, the results were found to be reproducible. The results for the two films are relatively similar, and only the measurements of 1 KΩ will therefore be given. The measurements were extended from 4.2K to 100mK using the oxford model 400 ^{3}He - ^{4}He dilution refrigerator.

Resistance and magnetoresistance measurements were made in the absence and the presence of a constant magnetic field of strength **B** = 4.0 T, with the samples mounted on the copper tabs to provide good thermal contact. The detailed usage of the dilution refrigerator is described elsewhere (Stoddart 1990). The resistance-temperature measurements were fitted to the Mott and the Efros-Shklovskii hopping laws. Most of the results fitted perfectly to the Efros-Shklovskii law, suggesting the presence of the CG and the random but stable distribution of localized energy states in space. The other results tend to follow the normal excitation of charge carriers to the conduction band. Figure 4.7 shows the sample resistances in the presence and absence of the magnetic field. A rise in the resistance of the sample in a magnetic field, although insignificant, was observed as a result of the strong localization of the energy states due to the shrinkage of carrier wavefunctions by the magnetic field.

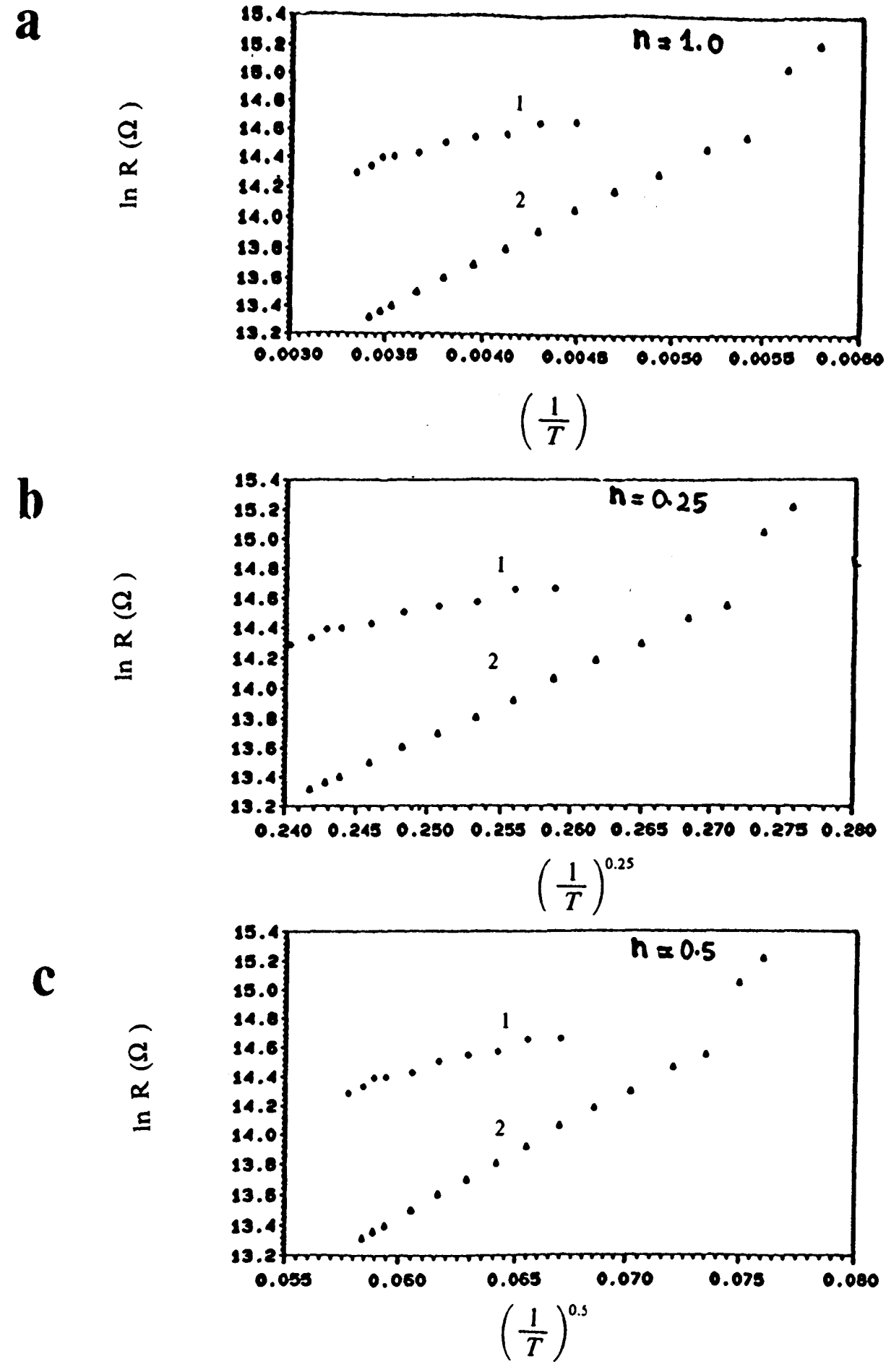


Figure 4.6 Plot of ln R (Ω) against $\left(\frac{1}{T}\right)^{n}$ for 2-point probe resistance measurements. Copper data are shown in diamonds (marked 1) and gold data are in triangles (marked 2).

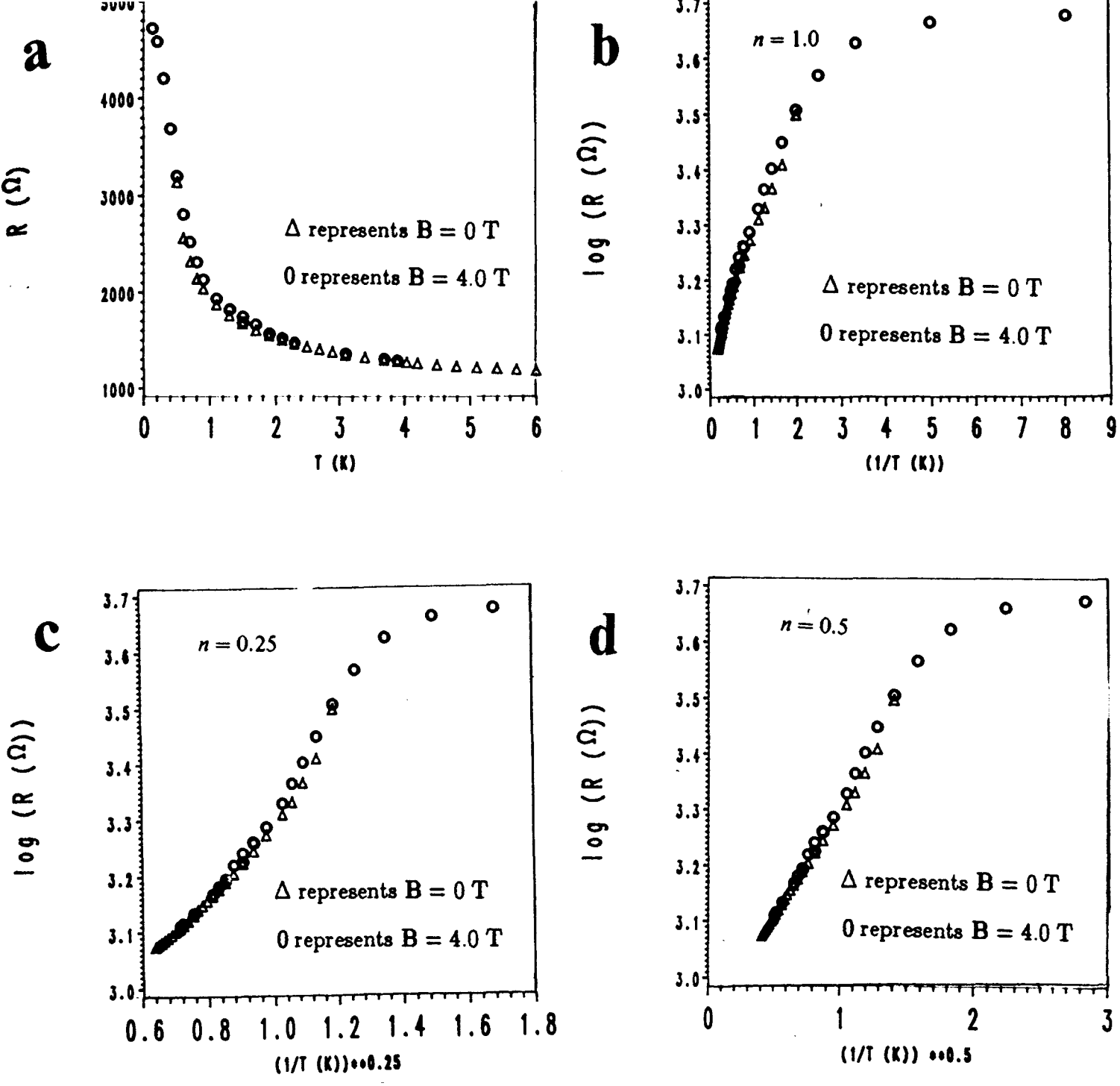


Figure 4.7 Plot of 1 KΩ ruthenium thin film resistors. (a) R Ω against T (*K*), (b)-(d) log R (Ω) against $T^{-n}(K^{-n})$

CHAPTER 5

Discussion of the Results

5.1 Introduction

This chapter contains an analysis of the low temperature resistance data presented in chapter 4. A theoretical model proposed by Prins *et al.* (1986) to describe hopping conduction in implanted surface layers of diamond is mentioned. The maximum hop distances between the graphitic clusters, assumed to be complex graphitic agglomerates, are approximated using the equation first proposed by Adkins (1989).

A detailed analysis for each measured diamond specimen is given in section 5.2. Section 5.3 is devoted to hopping conduction between the graphitic clusters, while excitations within the Coulomb gap are discussed in section 5.4. The two-point probe measuring technique is covered in chapter 5.5. A discussion of RuO_2 thin films is presented in section 5.6.

5.2 Sample Discussion

5.2.1 Sample 1 (Weak Hopper – $5.85 \times 10^{15} cm^{-2}$)

Two distinctive regimes (figure 4.3), separated by a fairly smooth change at 50 K, were observed in sample 1. It is very difficult to determine the exact form of the hopping conduction for this sample, as can be seen from figure 4.3. In the temperature range

50 K-4 K, the regression fitting method gives the value of $n = 0.07$ with a standard deviation of 0.265. The data fit fairly well to the Efros-Shklovskii VRH conduction theory in the temperature range 50K - 200 K, with a standard deviation of 0.533. The calculated n for the above temperature range was found to be 0.4. An exponent of unity in the hopping law is found to fit the data rather better than $n = 0.5$ and $n = 0.25$ in the temperature region 200 K- 300 K. At this temperature range, the most probable charge hopping mechanism is the excitation of electrons to the mobility edge, E_c, via the thermally activated processes (Miller and Abrahams 1960, Mott 1987). In this instance, with $n = 1.0$, eqn (4.1) describes the normal impurity conduction mechanism in which the activation energy ε_1 can be related to the characteristic temperature T_o by

$$\varepsilon_1 = kT_o = E_c - E_F \ , \tag{5.1}$$

where k is the Boltzmann's constant (Milligan *et al.* (1985)). At lower temperatures at which the VRH conduction, first suggested by Mott (1968), is likely to occur, the sample is believed to conduct via the phonon-assisted hopping between the neutral and ionized localized sites with an activation energy ε_3, resulting from the random fields of the dopant carbon ions. The general conductivity expression that accounts for the electrical conductivity in such a system is given by the equation

$$\sigma(T) = \sigma_1 e^{-\frac{\varepsilon_1}{kT}} + \sigma_2 e^{-\frac{\varepsilon_2}{kT}} + \sigma_3 e^{-\frac{\varepsilon_3}{kT}} + \sigma_{VRH} \ , \tag{5.2}$$

where $\sigma_1 = 1/\rho_1$, $\sigma_2 = 1/\rho_2$, and $\sigma_3 = 1/\rho_3$.

The energy ε_1, observed at high temperature, is the activation energy to the conduction band. The activation energy ε_2 is associated with an activation energy to the upper Hubbard band and thus with electron-electron interaction U. The activation energy ε_3 is attributed to an activation energy for hopping to an empty donor (acceptor) site in the presence of the singly occupied acceptor (donor) site. The identification of the three different processes is given by Fritzsche (1978).

5.2.2 Sample 2 (mild hopper - 5.70×10^{15} cm^{-2})

The hopping mechanism for sample 2 is studied sufficiently far away from the M-I transition on the insulating side. The results are summarized in figure 4.4. Over a temperature region 300 K-200 K a fixed nearest-neighbour hopping-type behaviour, as proposed by Miller and Abrahams (1960), takes place via the thermally assisted mechanism. A fit of $n = \frac{1}{2}$ in the semilog resistance plots tends to follow a straight line better than that of $n = \frac{1}{4}$. This is reflected in the χ^2 values of 0.261 and 0.904 for $n = 0.5$ and $n = 0.25$, respectively. This summarily suggests the possible existence of the CG and the presence of a strong electron correlation effect due to conduction electrons. A point worth noting is that, far away from the dilute limit of phase transition, the CG is smeared out as the band-gap narrows with the decreasing temperature. This implies that the effects of long-range Coulomb correlations become less effective due to the potential screening by the electrons.

The most probable assumption is a possible conductivity cross-over from Efros-Shklovskii to Mott hopping behaviour. This concept of cross-over is usually linked to the tentative theory of *hard gaps* which depends very strongly on the behaviour of the DOS near the electronic chemical potential (Vinzelberg *et al.* 1992, Zhang *et al.* 1990, Chicon *et al.* 1988). The occurrence of hard gaps has been observed experimentally in amorphous semiconductors (Voegele 1985) and other disordered systems (Vinzelberg 1992 and references therein). The theoretical results of hard gaps have been predicted by Davies (1985).

5.2.3 Sample 3 (strong Hopper - 5.65×10^{15} cm^{-2})

The strength of the electron correlation effect is determined by the number of interacting charge carriers in a disordered system. There is a significant reduction in electron interplay in sample 3, as depicted in figure 4.5. We only managed to make measurements

down to 50 K before the sample became too resistive to measure. A close comparison of the mild and strong hopper results, (figures 4.4 and 4.5) reveals the latter to be most likely to exhibit a possible conductivity cross-over, as is expected from the criteria advanced by Mott for the vanishing of the CG at very low temperatures. Pollak and Knotek (1979) have argued that the issue of CG is alleviated by a correlated multi-electron hopping mechanism at very low temperatures.

5.3 Hopping Conduction in Doped Semiconductors

A subtle theoretical model for charge hopping conduction in a doped diamond sample has been proposed by Prins *et al.* (1986). This addresses the situation for samples prepared using a cold-implantation-rapid-annealing (CIRA) cycle, during which the created self-interstitial atoms and vacancies diffuse through the damaged layer at preselected (high) temperatures. The model has been found to be applicable only above room temperature, in which Mott's VRH law is observed (Prins 1992). The charge conduction at high temperatures is suggested to take place through the vacloids sublattice structures. This model does not address the situation whereby the vacancies and the self-interstitials are severely impeded from diffusing through the substrate material. In fact, no consistent model exists yet for low temperature hopping phenomena (Graham *et al.* 1992, Abkemeier *et al.* 1992, Adkins 1989). One of the suggestions put forward by workers in this field, notably Hauser *et al.* (1977, 1976) and Adkins (1989), is that VRH in such systems involves graphitic bonds. The possibility of thermally activated hopping between complex conducting clusters (grains) cannot be excluded (Sheng *et al.* 1973).

5.4 Excitation in the Coulomb Gap

A thorough review of the excitations within the soft CG is given in papers by Pollak (1992) and Pollak and Ortuno (1985). The discussion in this section has been kept to a minimum due to paucity of the available information regarding the precise physical behaviour of the DOS within the CG. In fact, the method employed below to calculate the maximum hop distances between the conducting centres has been criticized previously. See Adkins (1989) and references cited therein.

In order to make a detailed quantitative comparison with the Efros-Shklovskii theory, we define the DOS for an interacting disordered system with the equation (Adkins 1989):

$$N(E) = \left(\frac{3^8 \pi^2 \varepsilon_r^3 \varepsilon_o^3}{2^5 e^6} \right) E^2 = g_{ES} E^2 \ , \tag{5.3}$$

where g_{ES} depends on the bulk relative permittivity, ε_r. The permittivity of diamond is $\simeq$5.7 (Field 1983). This gives $g_{ES} = 1.55 \times 10^{85}$ J^{-3}m^{-3}. g_{ES} is related to the tunnelling exponent α of the localized graphitic wavefunctions and the characteristic temperature by

$$kT_o = \frac{10.5\alpha}{(\pi g_{ES})^{1/3}} \ , \tag{5.4}$$

giving $\alpha = 6.53 \times 10^6$ m^{-1} (mild hopper) and $\alpha = 1.64 \times 10^8$ m^{-1} (strong hopper). The optimum hop distance is given by the equation

$$R_{opt} = \frac{0.25}{\alpha} \left(\frac{T_o}{T} \right)^{0.5} \ , \tag{5.5}$$

which can be evaluated at a particular temperature. The calculated R_{opt} values for mild and strong hoppers are given in table 5.1 below. Eqn (5.5) does not apply directly to a heavily doped sample.

T(K)	R_{opt} (nm) Mild hopper	R_{opt} (nm) Strong hopper
290	26.22	5.23
100	44.66	9.00
50	63.15	12.59

Table 5.1 Estimated optimum hop distances for mild and strong hoppers at different temperatures

The calculated R_{opt} values seem to be inconsistent with both the Efros-Shklovskii and Mott's theories. Reasonable values can be obtained where the critical doping concentration is known, in which the Mott criterion,

$$n_c^{1/3}\alpha^{-1} \simeq 0.26 \ , \tag{5.6}$$

will be used to determine α. The argument supporting this motion is presented by Abkemeier *et al.* (1992) for a hydrogenated amorphous $Si_{1-y}Ni_y$ material. The results obtained using the Miniut fitting computer program are summarized in table 5.2.

Ion dose $\times 10^{15}$ cm^{-2}	ΔT (K)	$R_{RT}(k\Omega)$	$R_o(k\Omega)$	T_o (K)	n	χ^2
5.70	290-4	17.054	9.12	136.05	0.5	0.261
5.65	290-50	848.37	27.2	3408.37	0.5	0.027

Table 5.2 Results of mild and strong hoppers that characterize the low temperature conductivity for a fixed value of $n = 0.5$.

5.5 Discussion of Two-point Probe Contact Measurements

Since different measuring devices were used to extract data, no definitive conclusion can be arrived at for the two-point probe contact measurements. Our principle objective, as stated previously, was to link up with Prins' (1992) measurements for the same diamond samples which exhibited the VRH conduction described by the Mott $T^{-1/4}$ law, at high temperatures. An unusual rise in the resistance measurements was noticed in the case of the copper contacts as opposed to the gold contacts, as revealed in plots of log(*Res*) against $T^{-1/2}$ and $T^{-1/4}$. Both plots fitted reasonably well to both forms of conduction, except for high temperature measurements. This makes it difficult to postulate the true mechanism of charge conduction. It has been suggested that not only the diamond resistance was measured but also that of the contacts. The gold contacts were found to behave linearly (stable) over the whole temperature range. This makes them suitable for future experiments.

5.6 Discussion of RuO_2 Results

Two nominal RuO_2 thin films were studied both in the absence and in the presence of a magnetic field of strength **B** = 4.0 T. An overview report of these films is given, since measurements are of secondary concern in this research report. The results of 30 KΩ films are relatively the same as that of 1 KΩ thin film, and only the latter measurements will therefore be discussed. Two distinctive regions, separated by a smooth shoulder, were observed for the 1 KΩ nominal film. Measurements made from 300 K down to 100 K fitted well to $n = \frac{1}{2}$ and from 100 K - 4 K a slope of $n = 1.0$ was obtained. For the following temperature range 4 K to 0.1 K, a slope of $n = \frac{1}{2}$ tends to fit the data better than that of $n = 1.0$. Measurements carried out in the absence and presence of a magnetic field are shown in table 5.3.

ΔT (K)	n	T_o (K)	$R_o(\Omega)$
100-4	1	1.272	982.5
4-0.5	0.5	0.641	938.4

Table 5.3 Summary of adjustable parameters calculated at different temperatures for 1 KΩ ruthenium oxide specimen.

An insignificant rise in the resistance for the 1 KΩ ruthenium oxide specimen was observed. The results are plotted on the same scale as those in the absence of the field for comparison purposes, and are shown in figure 4.7.

CHAPTER 6

Summary and Conclusion

The basic aim of this research project was to investigate the possible occurrence of the metal insulator transition in heavily carbon-ion implanted type IIa diamonds at low temperatures. In particular, we set out to establish whether Mott or Efros-Shklovskii variable range hopping conduction applies in implanted diamond samples and nominal ruthenium 'oxide thin films at low temperatures. Implanted diamond samples with ion doses 5.65×10^{15} cm^{-2} referred to as strong hopper, 5.70×10^{15} cm^{-2} mild hopper and 5.85×10^{15} cm^{-2} weak hopper and RuO_2 films of resistance 1 KΩ and 30 KΩ at room temperature were studied using four- and two-lead measuring techniques. RuO_2 film measurements were extended to $\simeq$100 mK using the ^{3}He-^{4}He dilution refrigerator.

6.1 Type IIa Diamond Results

It has been observed that, far removed from the metal insulator transition on the insulating side of the transition, the results of strong and mild hoppers tend to fit the Efros-Shklovskii VRH better than the Mott $T^{-1/4}$ law over the entire temperature range. A conductivity cross-over is envisaged for these samples, as reflected in figures 4.4 and 4.5. This is due to the fact that at sufficiently low temperatures, at which the DOS can be regarded as constant and nonvanishing, hopping conduction results from localized states with energies close to kT in a narrow band near the electronic chemical potential (Fermi level). These states lie far away from each other and can be presumed to be

spatially uncorrelated. In this case the contribution due to the effects of electron correlations can therefore be neglected. These are in fact the conditions put forward by Mott in deriving his $T^{-1/4}$ law.

For a sample near the M-I transition, fixed range hopping conduction, (as outlined by Miller and Abrahams (1960) dominates over a large temperature range. No firm conclusions can be drawn from the $T^{-1/2}$ and $T^{-1/4}$ plots, as shown in figure 4.3.
In the case of the two-lead measurements, it is believed that not only the sample resistance was measured but also that of the contacts. Gold contacts were found to be more stable than copper contacts. They are therefore more suitable for use in future measurements.

RuO_2 Thin Film's Results

An index factor close to 1/2 was obtained in both nominal ruthenium oxide films over a temperature range of 160 K - 0.1 K, suggesting the existence of strong electron-electron interaction and the presence of the Coulomb gap in the VRH regime. An impurity conduction describes the temperature region 300 K - 160 K.
Concerning future trends, further work at low temperatures, including magnetoresistance and Hall effect measurements, may shed more light on the nature of the conducting centres. Similar work on boron implanted diamond is also of potential interest.

References

(1) Abkemeier, K.M., C.J. Adkins, R. Asal and E.A. Davies, 1992, Phil. Mag. **B65**, 675

(2) Abrahams, E., P.W. Anderson, D.C. Licciardello, and T.V. Ramakrishnan, 1979, Phys. Rev. Lett. **42**, 693

(3) Adkins, C.J., 1989, J. Phys. Condensed Matter, **1**, 1253

(4) Ambegaokar, V., B.I. Halperin, and J.S. Langer, 1971, Phys. Rev. **B4**, 261

(5) Anderson, P.W., 1958, Phys. Rev **109**, 1492

(6) Baranovskii, S.D., A.L. Efros, B.L. Gelmont and B.I. Shklovskii, 1979, J. Phys. **C12**, 1023

(7) Berggren, K.-F, and B.E. Sernelius, 1985, Solid State Electronics **28**, 11

(8) Bosch, W.A., F. Mathu, H.C. Meijer, and R.W. Willekers, 1986, Cryogenics **26**, 3

(9) Bottger, H., V.V. Bryksin, 1985, *Hopping Conduction in solids*, VCH Publishers.

(10) Brenzini, A., N. Zekri, 1992, Phys. Stat. Sol. (b) **169**, 253

(11) Castner, T.G., 1991, p1 in *Hopping Transport in Solids* edited by Pollak, M. and B.I. Shklovskii, Elsevier Science Publishers B.V., Netherlands.

(12) Chicon, R., M. Ortuno, M. Pollak, 1988, Phys. Rev. **B37**, 10520

(13) Davies, J.H., P.A. Lee, and T.M. Rice, 1982, **B29**, 4260

(14) Davies, J.H., 1985, Phil. Mag. **B52**, 511

(15) Davies, J.H., J.R. Franz, 1986, Phys. Lett **57**, 475

(16) Derry, T.E., 1980, PhD Thesis, University of the Witwatersrand

(17) Derry, T.E., C.C.P. Madiba, J.P.F. Sellschop, 1983, Nuclear Instrum. Methods **218**, 559

(18) Edwards, P.P., M.J. Sienko, 1978, Phys. Rev. **B17**, 2573

(19) Efros, A.L. and B.I. Shklovskii, 1975, J. Phys. **C8**, L49

(20) Efros, A.L. and B.I. Shklovskii, 1985, chapter 5, 409, in *Electron-Electron Interactions in Disordered Systems* ed. Efros, A.L. and M. Pollak. Elsevier Science Publishers B.V., Netherlands.

(21) Field, J.E., 1992, *The Properties of Natural and Synthetic Diamond* p684, Acedemic Press, Cambridge

(22) Fritzsche, H. 1978, p 193, in *The Metal-Non Metal Transitions in Disordered Systems*, edited by Friedman, L.R., and Tunstall, D.P., SUSSP Publications, Edingburg

(23) Fukuyama, H. 1985, chapter 2, 155, in *Electron-Electron Interactions in Disordered Systems*, edited by Efros, A.L. and M. Pollak. Elsevier Science Publishers B.V., Netherlands.

(24) Graham, M.R., J.R. Bellingham and C.J. Adkins, 1992, Phil. Mag. **B65**, 669

(25) Hauser, J.J., J.R. Patel and J.W. Rodgers, 1977, Appl. Phys. Lett. **30**, 129

(26) Hauser, J.J. and J.R. Patel, 1976, Solid State Commun. **18**, 789

(27) Hill, R.M., 1976, Phys. Stat. Sol. **A35**, K29

(28) Hill, R.M. and A.K. Jonscher, 1979, J. Non-Crystalline Solids **32**, 53

(29) Holinger, G., P. Pertosa, J.P. Doumerc, F.J. Humpsel and B. Reichl, 1985, Phys. Rev. **B32**, p 1987

(30) Kane, E.O., 1985, Solid State Electronics, **28**, 3

(31) Kawabata, A., 1980, J. Phys. Soc. Japan Suppl. **A49**, 375

(32) Kurosawa, T. and H. Sugimoto, 1975, Prog. Theor. Phys. Suppl. **57**, 217

(33) Levin, E.I., B.I. Shklovskii and A.L. Efros, 1987, Sov. Phys. JETP **65**, 842

(34) Li, Q., C.H. Watson, R.G. Goodrich, D.G. Haase and H. Lukefahr, 1986, Cryogenics **26**, 467

(35) Mayer, J.W., L., Eriksson, and J.A. Davies, 970, *Ion Implantation in semiconductors: silicon and germanium* Acedemic Press, New York

(36) McMillan, W.L. and J. Mochel, 1981, Phys. Rev. Lett **46**, 556

(37) Miller, A. and E. Abrahams, 1960, Phys. Rev. **120**, 745

(38) Milligan, R.F., T.F., Rosenbaum, R.N. Bhatt and G.A. Thomas, chapter 3, 231, in *Electron-Electron Interactions in Disordered Systems* edited by Efros, A.L. and M. Pollak. Elsevier Science PublishersB.V., Netherlands.

(39) Mobius, A., 1985, J. Phys. Solid State **C18**, 4639

(40) Mochena, M. and M. Pollak, 1991a, Phys. Rev. Lett **65**, 109

(41) Mochena, A. and M. Pollak, 1991b, J. non-crystalline solids **131-133**, 1260

(42) Monroe, D., 1991, p49, in *Hopping Transport in Solids* edited by Pollak, M. and B.I. Shklovskii, Elsevier Science Publishers B.V., Netherlands.

(43) Mott, N.F., 1967, Adv. Phys. **16**, 49

(44) Mott, N.F., 1968, J. non-crystalline solids **1**, 1

(45) Mott, N.F., 1974, *Metal Insulator Transitions* 1st ed (Taylor and Francis, London).

(46) Mott, N.F., 1975a, J. Phys. **C8**, L49

(47) Mott, N.F., 1975b, J. Phys. **C8**, L239

(48) Mott, N.F., 1978, p149, in *The Metal Non-Metal Transition in Disordered Systems* edited by Friedman, L.R. and D.P. Tunstall

(49) Mott, N.F., 1987, *Conduction in Non-Crystalline Materials* , Oxford University Press.

(50) Mott, N.F., 1989, Phil. Mag. **B60**, 365

(51) Mott, N.F., 1990, *Metal Insulator Transitions* 2nd edition, Taylor and Francis, London

(52) Mott, N.F. and M. Kaveh, 1985, Phil. Mag. **52**, 177

(53) Nag, B.R., 1980 *Electrical Properties in Compound Semiconductors*, **11**, Springer series in Solid State Sciences.

(54) Ortuno, M. and J. Ruiz, 1992, Phil. Mag. **B65**, 647

(55) Pantelides, S.T., A.Selloni and R. Car, 1985, Solid State Electronics, **28**, 17

(56) Pollak, M., 1971, Phil. Mag. **23**, 519

(57) Pollak, M. and M.L. Knotek, 1979, J. non-crystalline solids **32**, 141

(58) Pollak, M. and M. Ortuno, 1985, Chapter 4, p287, in *Electron-Electron Interactions in Disordered Systems*, edited by Efros A.L. and M. Pollak. Elsevier Science Publishers B.V., Netherlands.

(59) Pollak, M. and A. Hunt, 1991, p175, in *Hopping Transport in Solids*, edited by Pollak, M. and B.I. Shklovskii

(60) Pollak, M., 1992, Phil. Mag. **B65**, 657

(61) Prins, J.F., 1985, Phys. Rev. **B31**, 781

(62) Prins, J.F., T.E.. Derry, J.P.F. Sellschop, 1986, Phys. Rev. **B34**, 8870

(63) Prins, J.F., 1988a, Phys. Rev. **B38**, 5576

(64) Prins, J.F., 1988b, Nucl. Instrum. Methods **B35**, 484

(65) Prins, J.F., 1989, Phys. Rev. **B39**, 3764

(66) Prins, J.F., 1991, Phys. Rev. **B44**, 2470

(67) Prins, J.F., 1992, Material Science Report **7**, 271

(68) Rosenbaum, T.F., K. Andres, G.A. Thomas and R.N. Bhatt, 1980, Phys. Rev. Lett. **45**, 1723

(69) Ryssel, H. and I. Ruge, 1986, *Ion Implantation* (Wiley, New York)

(70) Sawicka, B.D., J.A. Sawicki, H. de Waard, 1981, Phys. Lett **A85**, 303

(71) Schiff, L.I., 1968, *Quantum Mechanics*, p314 , 3rd edition, McGraw-Hill, Inc

(72) Sheng, P, B. Abeles and Y. Arie Phys. Rev. Lett. 1973, **31**, 44

(73) Shklovskii, B.I. and A.L. Efros, 1984, *Electronic Properties of Doped Semiconductors*, **45**, Springer Series in Solid State Sciences

(74) Spitz, R.A., 1990, MSc Thesis, University of the Witwatersrand

(75) Srinivasan, G., 1971, Phys. Rev **B34**, 2581

(76) Stoddart, S.T., 1990, MSc thesis, University of the Witwatersrand

(77) Thouless, D.J., 1978, p61, in *The Metal Non-Metal Transition in Disordered Systems*, edited by Friedman, L.R. and D.P. Tunstall.

(78) Van Mieghem, P., 1992, Rev. Modern Phys. **64**, 755

(79) Vandersande, J.W., 1976, Phys. Rev. B13 , 4560

(80) Vavilov, V.S., M.I. Guseva, E.A. Konorova and V.F. Sergienko, 1970, Sov. Phys. Semicond. **4**, 6; see also page 12 of the same journal.

(81) Vavilov, V.S., 1975 , Phys. Stat. Sol. **31a**, 11

(82) Vinzelberg, H., A., Heinrich, C., Gladun and D. Elefant, 1992, Phil. Mag. **B65**, 651

(83) Vetterling, W.T., S.A. Teukolsky, W.H., Press and B.P. Flannery, 1988, *Numerical Recipes*, Cambridge University Press, U.S.A.

(84) Voegele, V., S. Kalbitzer and K. Bohringer, 1985, Phil. Mag. **B52**, 153

(85) White, H., 1988, PhD thesis, University of the Witwatersrand

(86) Williams, A.W.S., E.C. Lightowlers and A.T. Collins, 1970, J. Phys. **C8**, 1729

(87) Wolf, E.L., R.H. Wallis and C.J. Adkins, 1975, Phys. Rev. **B12**, 1603

(88) Zabrodskii A.G., 1977, Sov. Phys. Semicond. **11**, 345

(89) Zabrodskii, A.G., 1981, Sov. Phys. JETP Lett **33**, 243

(90) Zabrodskii, A.G. and K.N. Zinove'va, 1984, Sov. Phys. JETP **59**, 425

(91) Zhang, Y, P. Dai, M. Levy and M.P. Sarachik, 1990, Phys. Rev. Lett **64**, 2687

APPENDIX

Fortran computer programs used to analyze the data are presented below. Programs, listed in their order of executions, *viz: Tmott slope intercept, LnW and LnT generator,* and *check theory and expt*, can be run separately by RUNVA EXEC, or simultaneously by G EXEC. To use RUNVA EXEC, enter RUNVA in the CMS running mode and follow the instructions. For the executions of files using G EXEC, enter g in the cms mode.

The results obtained in the above programs were calculated (or verified) using the MINUIT FITTING program. The latter program is run by COUL EXEC, and instructions are followed. To enter the data files (as specified) type COULPAR *name of the data file to be analyzed* TERM. The values of R_o, T_o and n can be varied or fixed in our pursuit to increase the precision of the above parameters and to reduce the errors (given by chis in the program).

PROGRAM ln W and ln T generator

```
        PROGRAM LnW and lnT generator

$DECLARE
$DEBUG
$NOTRUNCATE

*****************************************************************
*The resitivity and temperature taken during experimemtal       *
*                                                               *
*runs are transformed into ln W and ln T.this data is then      *
*                                                               *
*used to calculate the slope the Mott characteristic temp.      *
*                                                               *
*****************************************************************

         implicit real*8 (a-h,o-$),integer (i-n)
         integer ndata
         Parameter(ndata=27  )

         integer i
         real*8  xdata(ndata),ydata(ndata),x(ndata),y(ndata)
         real*8  avetemp(ndata),tempdiff(ndata),delnR(ndata),W(ndata)
         real*8  calldata(ndata),dialdata(ndata),R(ndata)

         do 5 i=1,ndata

               read(5,*)x(i),y(i) !x(i)=temp values
               xdata(i)=x(i)
               ydata(i)=dlog(y(i))  !y(i)= resistivity

5        continue

         write(14,*)'data is analysed from the temperature range of '
         write(14,*)'  '
         write(14,2)x(1),x(ndata)
         write(14,*)'
         write(14,*)'and the resistivities corresponding to the temps '
         write(14,*)'  '
         write(14,9000)y(1) ,y(ndata)

2        format(2x,2F13.4,2x,E13.5)
9000     format(2x,2E13.4,2x,E13.5)

         DO 100  i=2,ndata-1

              tempdiff(i)=x(i)-x(i-1)
              avetemp(i)= (x(i) +x(i-1))/2.0d0
              delnR(i)=ydata(i)-ydata(i-1)
              W(i)=-avetemp(i)*delnR(i)/tempdiff(i)


          If (W(i).lt.0.0)  GOTO 100

              dialdata(i)=dlog(W(i))
              calldata(i)=dlog(avetemp(i))


c          If (delnR(i).lt.0.0.and.y(i).gt.y(i-1)) goto 1
1           WRITE(15,90) x(i),y(i)
90          FORMAT(2x,1F12.5,6x,2E17.7)
```

```
            write(4,9)calldata(i),dialdata(i)
9           format(2x,2E23.5)
100         CONTINUE
                call exit
                end
```

PROGRAM Tmott slope intercept

```
                PROGRAM Tmott slope intercept
*****************************************************************
* The program calculates the slope(exponential factor) in the   *
*                                                               *
* resistivity equation, the Mott characteristic temperature     *
*                                                               *
* and the intercept.The values used are generated by Trtr       *
*                                                               *
* fortran: ln W and ln T. For convinence the two program are    *
*                                                               *
* kept separately.                                              *
*                                                               *
*****************************************************************

$DECLARE
$DEBUG
$NOTRUNCATE

          IMPLICIT REAL * 8 (A-H,O-Z),INTEGER (I-N)

          integer ndata,i,nout

          parameter(ndata = 36     )


          real     b0,b1,d(ndata),f(ndata),r(ndata),temp(ndata)

*****************************************************************
*                                                               *
* the parameters used below are from the cms/imsl routines.     *
*                                                               *
*****************************************************************

          real   stat(12)
          character clabel(13)*15,rlabel(1)*4
          external rline,umach,wrrrl
       data rlabel/'none'/,clabel/' ','mean of x','mean of y','variance
      .   x','variance y','corr.','std.err. b0','std.err. b1','df reg.',
      .   'ss reg.','df error','ss error','pts with nan'/

*****************************************************************
* read now below ln W and ln T calculated from trtr fortran     *
*                                                               *
* (d(i) & f(i) respectively.                                    *
*                                                               *
* we use a subroutine (cms) to calculate slope,etc              *
*                                                               *
*****************************************************************


          do  i=1,ndata

              read(5,*)d(i),f(i)
          enddo
```

```
          call rline(ndata,d,f,b0,b1,stat)

            Tmott= (-1/b1*2.718281828**(b0))**(-1/b1)

         write(8,*) ' '
            write(8,9)b0,b1,Tmott
*           write(12,999)b0,b1,Tmott
999    format(2x,1e8.2,3x,1e12.2,3x,e13.2)
9      format(//'intept=',e12.2,//,'slope=',e12.2,//,'Tmott=',e13.2,//)

         call umach(2,nout)
         call wrrrl('%/stat',1,12,stat,1,0,'(12w10.4)',rlabel,clabel)
         call exit

            end

*****************************COMMENTS*********************************

*stat(12)=vector oflength 12 with statistics below
*external rline,umach,wrrrl=cms subroutines
*b0,b1=estimated intercept & slope of fitted line respectively.
*from rlabel: 1-12 stat
*1-7 need no explation
*8=degree of freedom for regression
*9=sum of squares for regression
*10=degree of freedom for error
*11=sum of squares for error
*12=#of (x,y)points containing nan(not a number)as either the
*x or y values.
```

PROGRAM Check theory and expt

```
      PROGRAM Check theory and expt

$DECLARE
$DEBUG
$NOTRUNCATE

*************************************************************
* The program takes on the values of slope and To, to       *
*                                                           *
* generate the theoretical values, using average Ro value   *
*                                                           *
* (see compare data) after running the program.             *
*                                                           *
*************************************************************

      implicit real*8(a-h,o-$)
         integer i,ndata
        parameter (ndata= 22  )
           real*8 R(ndata),t(ndata),Ro(ndata),res(ndata)
             real Tmott,slope,Roave

      READ(12,*)intercept,slope,Tmott
      Roave=0.0d0

      write(6,*)'   Ro values    res(experimental)'
    write(3,*)'The theoretical values are generated using Ro values.'
    write(3,*)'The latter is obtained from the resistivity equation:'
    write(3,*)' '
    write(3,*) 'R(T)=Ro exp(To/T)**x'
    write(3,*)'where x is the determined slope. Refer to Ro_Res data'

      write(3,*)'  '
     write(3,*)'    Temp(K)   res(theoretical)  res(experimental)'
     write(3,*)' '

      do i=1,ndata

       read(5,*)T(i),R(i)
         Ro(i)=R(i)/(2.71828183**(Tmott/T(i))**(-slope))
           R(i)=Ro(i)*(2.71828183**(Tmott/T(i))**(-slope))
             Roave=Roave+Ro(i)
                roave1=roave/ndata

      write(6,2)Ro(i),R(i)
2     format(2x,e12.5,3x,e14.5)
      enddo

      write(6,*)' '
       write(6,*)' '
        write(6,*)'average Ro value'
         write(6,2)Roave1
          write(6,*)' '

      do i=1,ndata

        Res(i)=Roave1*(2.71828183**(Tmott/T(i))**(-slope))
         write(3,9)T(i),Res(i),R(i)
9         format(f12.4,3x,e13.4,2x,e14.4)

    enddo

      call exit
      end
```

RUNVA

```
    /** RUNVA : exec to run Fortran programs  **/
    Parse upper arg fnf fnd fno
    Select
     When fnf='' then do
                      say;say ' Enter name of Fortran text file.';parse upper pull
fnf
                      say;say ' Enter name of data file.';parse upper pull fnd
                      say;say ' Enter name of output file.';parse upper pull fno
                      end
     When fnd='' then do
                      say;say ' Enter name of data file.';parse upper pull fnd
                      say;say ' Enter name of output file.';parse upper pull fno
                      end
     When fno='' then do
                      say;say ' Enter name of output file.';parse upper pull fno
                      end
     Otherwise nop
    End
    'FILEDEF 5 DISK' fnd 'DATA A (PERM'
    'FILEDEF 6 DISK' fno 'DATA A (PERM'
    'EXEC FORTG' FNF
     rcfortg = rc
    'FILEDEF FT05F001 CLEAR'
    'FILEDEF FT06F001 CLEAR'
     Exit rcfortg
```

G EXEC

```
/*The programs: trtr, tru and comb are executed by typing g in the*/
/*cms mode*/

'fortc trtr '
'fi 5 disk RuO_4t   data '       /**<<<<<< change here <<<<<**/
'fi 4 disk lnW_lnT data '
'fi 6 disk keep  data '
/*******'fi 35 disk gordon  data '**********/
' fi 14 disk temp_res data'

'fortg trtr'
'erase trtr text'
'erase trtr listing'
'erase keep data'
/**/

'fortc tru'
'fi 1 disk ndata    data '
'fi 5 disk lnW_lnT  data '
'fi 12 disk Int_s_To data'
'fi 8  disk answer  data '
'fi 6 disk std_devn  data '
'fortg tru'
'erase  tru text'
'erase tru listing'
/**/

'fortc comb'
'fi 5 disk RuO_4t  data '        /**<<<<CHANGE HERE<<<<****/
'fi 3  disk compare  data '
'fi 12 disk Int_s_To  data '
'fi 6 disk ro_res data '

/***********'fi 1 disk Iam_best data'***************/
'fortg comb'
'erase  comb text'
'erase comb listing'
'x int_s_To data '

'x answer data '
'x compare data '
'x lnW_lnT  data '
'x temp_res data'
'x ro_res data '
/**/
```

MINUIT FITTING PROGRAMS

```
C     ****************************************************************
C     ****************************************************************
C     * PROGRAM TO FIT T R DATA TO THE COULOMB_GAP EQN               *
C     *      R=R0*EXP((Tc/T)**n)                                     *
C     ****************************************************************
c     ****************************************************************


      SUBROUTINE FCN(NPAR,GPAR,CHIS,PAR,IFLAG)
      IMPLICIT REAL * 8(A-H,O-Z)
      DOUBLEPRECISION XE(900),YE(900)
      DOUBLEPRECISION T,RE,TC,RC,R0,CHIR,CHIS,EXPN,TMIN
      DOUBLEPRECISION RMIN,RMAX,RLEAK,RES,offset,tlre,tlrc
      REAL*8 MMPSI
      DIMENSION PAR(8),GPAR(1)
      INTEGER N,NDATAE
      REAL FLAG
      R0=10.0**PAR(1)
      TC=PAR(2)
      EXPN=PAR(3)
      offset=par(4)
      TMAX=PAR(5)
      RMIN=10.0**PAR(6)
      RMAX=10.0**PAR(7)
      RLEAK=10.0**PAR(8)

C ***************************************************************************
      IF(IFLAG.NE.1) GOTO 30
C     WRITE(6,171)
      READ(5,*) FACTOR
C     factor=1.0
      READ (5,*) NDATAE
      Ngood=0
      DO 211 N=1,NDATAE
         READ (5,*) XE(N),YE(N)
         IF (YE(N).LT.RMAX.AND.YE(N).GT.RMIN) then
           Ngood=Ngood+1
           XE(Ngood)=XE(N)
           YE(Ngood)=YE(N)
         ENDIF
C    *      YE(Ngood)=Rleak*YE(Ngood)/(Rleak-YE(Ngood))
C        WRITE(6,112) N,XE(N),YE(N)
  211 CONTINUE
      NDATA=Ngood
   30 CHIS=0.0D0
      CHIR=0.0D0
c     IF (iflag.eq.3) write(6,35) 10.0**R0
   35 FORMAT(1x,'R0 = ',F12.4)
      DO 42 N=1,NDATA
         RE=YE(N)/FACTOR
       tlre=log10(re)
         T=XE(N)
c        IF (t.lt.tmax) then
           RC=R0*EXP((Tc/T)**EXPN)
       tlrc=log10(rc)
           CHIR=tlre-tlrc
           CHIS=CHIS+CHIR**2
```

```
            IF (IFLAG.EQ.3)THEN
               WRITE(6,22) T,RE,RC,chir,chis
            ENDIF
c         endif
   42 CONTINUE
      RETURN


C                  FORMAT STATEMENTS
  100 FORMAT (I3)
  112 FORMAT (1x,I3,' : ',2F15.5)
   22 FORMAT (1X,1F8.3,2E25.6,1x,2F14.6)
  171 FORMAT (1X,' N          TEMP.          RES.')
C  50 FORMAT (1X,' Finnished Reading in data ')
C  51 FORMAT (1X,'Exp : ',F10.4,'  F(',F10.4,')=',F10.4)
      END
```

COUL EXEC

```
/*****************************************************************
***                                                            ***
***     COUL : REXX exec to submit several data files to MINUIT ***
1  ***               A maximum of 5 data files can be specified  ***
***               The exec also writes data to a file which can ***
***               be processed by a SAS program .              ***
*****************************************************************/
Address CMS
Signal on halt
Narg=arg()
Call setup
Select
When narg=0 then do
                call getfunc
                call getdata
                end
       otherwise do
                parse upper arg files
                ndata=words(files)-1
                parse var files func data1 data2 data3 data4 data5 .
                if func='?' then call explain
                if data1='' then call explain
                call findfunc
                call finddata
                end
End
  Do n=1 to ndata
  file=value(data||n)
  'Copy ' file ' data a temp data d (app'
  End n
Say;say '  Do you want to look at the combined file (Y/N)?   Default is N.'
Parse upper pull ans 2 .
If ans='Y' then 'xedit temp data d'
Say;say '  Enter heading for this run.'
Say;say '  QQ will erase the temporary file & abandon the run.'
Parse pull heading
If heading='QQ' then call exitt
Nameit:
say;say 'Enter Filename for run :'
Parse upper pull fn
'Set CMSTYPE HT'
'State' fn 'DATA D'
retc=rc
'Set CMSTYPE RT'
If retc=0 then do
               say;say '  ' fn 'DATA D already exists.'
               say '  Overwrite it (Y/N)?   Default is Y.'
               parse upper pull ans 2 .
               if ans='N' then do
                               say '  Try another name.'
                               signal nameit
                               end
                          else 'erase' fn 'DATA D'
               end
'Set CMSTYPE HT'
'fi 5 disk temp data d'
'fi 6 disk ' fn ' data d'
'EXEC FORTG MINUITS ( TEXTS ' func
'execio 1 diskw' fn 'data d (string'
```

```
'execio 1 diskw' fn 'data d (string  ' heading
'execio 1 diskw' fn 'data d (string   Run on        :
'dayr dater 'at' timer
'execio 1 diskw' fn 'data d (string   Function used : ' func
'execio 1 diskw' fn 'data d (string   Data File(s)  :
'data1 data2 data3 data4 data5
Say '  ' heading
Say '   Run on        : ' dayr dater 'at' timer
Say '   Function used : ' func
Say '   Data file(s)  : ' data1 data2 data3 data4 data5
Say
Files:
say;say 'Would you like the file stripped ? (Y/N)'
parse upper pull ans 2
say 'in runriq FN=' fn
if ans='Y' then 'strip' fn 'data d'
'Xedit' fn 'DATA D'
Say;say '  Do you want the file printed (Y/N)?   Default is N.'
Parse upper pull ans 2 .
If ans='Y' then do
      say;say '  Print in Physics (P) (default) or Computer Centre (C) ?'
               parse upper pull ans 2 .
               if ans='C' then 'PRINTER 2 1 '
                          else do
                               'CP SP P RSCS'
                               'CP TAG DEV E PHYPRT1'
                               end
               'Print ' fn 'DATA D (LINECOUN 62'
               'CP PRINT'
               end
Say ' '
say 'Do you want the file erased (Y/N)? .To have the data arranged
 for plotting      enter N. Default is Y.'
Parse upper pull ans 2 .
If ans='N' then nop
           else 'erase' fn 'DATA D'
if ans='Y' then call exitt
Say;say '  Do you want to have the file saved for plotting (Y/N)?'
Parse upper pull ans 2 .
if ans='Y' then do
STRING1='a'
STRING2='z'
do until COMPARE(STRING1,STRING2)=0
'execio 1 diskr'  fn DATA 'D 0 (var LINE'
STRING1=substr(LINE,18,9)
STRING2='IFLAG = 3'
end
do until substr(LINE,12,9)='Execution'
'execio 1 diskr' fn 'DATA D (var LINE'
if substr(LINE,12,9)='Execution' then nop
else if substr(LINE,1,132)='                              ' then nop
else 'execio 1 diskw' fn 'PLOT A (string' line
end
'finis fn DATA D'
'finis fn PLOT A'
end
Call exitt
/*****   sets up constants etc.                          *****/
Setup:
```

```
Dayr=Date(w);dater=date()
Timer=Time();timer=substr(timer,1,5)
notfnd=0
'Set CMSTYPE HT'
'State temp data'
If rc=0 then 'erase temp data'
'Set CMSTYPE RT'
m.1=jan;m.2=feb;m.3=mar;m.4=apr;m.5=may;m.6=jun
m.7=jul;m.8=aug;m.9=sep;m.10=oct;m.11=nov;m.12=dec
Return
/*****   explain the usage                          *****/
Explain:
Say;say '  Enter EITHER : RUNMA function datafile1 ..... datafile5'
Say '         OR      : RUNMA   (and you will be prompted for your input).'
Say;say '  Now try again';say
Exit 0
/*****   gets function file                         *****/
Getfunc:
Say;say '  Enter function filename'
Say;say '  QQ will end the run.'
Parse upper pull func .
If func='QQ' then call exitt
Call findfunc
Return
/*****   checks existence of function file          *****/
Findfunc:
'Set CMSTYPE HT'
'State' func ' TEXT *'
retc=rc
'Set CMSTYPE RT'
If retc¬= 0 then do
                 say;say '   ' func 'TEXT * does not exist,- try again.'
                 call getfunc
                 end
Return
/*****   gets data files                            *****/
Getdata:
Say;say '  Enter data filename(s)  (1-5 can be entered).'
Say '  They must be on ONE line, separated by blanks.'
Parse upper pull datafiles
ndata=words(datafiles)
Parse var datafiles data1 data2 data3 data4 data5 .
Call finddata
Return
/*****   checks existence of data file(s)           *****/
Finddata:
notfnd=0
Do n=1 to ndata
'Set CMSTYPE HT'
file=value(data||n)
'State' file ' DATA *'
retc=rc
'Set CMSTYPE RT'
If retc¬= 0 then do
                 say;say '   ' file 'DATA * does not exist.'
                 notfnd=1
                 end
End n
if notfnd=1 then do
```

```
                say;say '  You must enter the WHOLE data list again.'
                call getdata
                end
  Return
  /*****   tidies up after user termination          *****/
  Halt:
  Say;say '*****   RUN TERMINATED BY USER   *****'
  'CP sp cons stop close'
  Call exit
  Return
  /*****   exits cleanly                             *****/
  Exitt:
  'Set CMSTYPE HT'
  'Erase temp data d'
/*'Rel B (det'*/
  'Set CMSTYPE RT'
  Exit 0
  /*****   end of exec                               *****/
```

COULPAR DATA

Coulomb	***** 6,7,8 in GOhms ******					
	1	R0(log)	00.0	0.5	-15.0	15.0
	2	T0	10000.	100.0	10.0	9999999.
	3	n	1.0	0.02	0.0	1.0
	4	Offset	0.0	0.0	0.0	20.0
	5	Tmax	40.0	0.0	0.0	200.0
	6	RMin-log	2.0	0.0	0.0	12.0
	7	RMax_log	15.0	0.0	0.0	14.0
	8	RLeak	15.0	0.0	0.0	16.0

TERM DATA

```
PRINTOUT   3
FCN        3
MIGRAD
FCN        3
EXIT
```